IEEE Access
Multidisciplinary | Rapid Review | Open Access Journal

Received 22 April 2025, accepted 8 May 2025, date of publication 16 May 2025, date of current version 30 May 2025.

*Digital Object Identifier 10.1109/ACCESS.2025.3570719*

RESEARCH ARTICLE

# Dynamic Modeling and Quantum-Enhanced Forecasting of Multi-Seasonal Energy Prices in Simulated Microgrid Environments

**RITESH DASH[1], ANUPA SINHA[1], K. JYOTHEESWARA REDDY[2], C. DHANAMJAYULU[3], (Senior Member, IEEE), AND INNOCENT KAMWA[4], (Fellow, IEEE)**

[1]Computer Science Engineering, Kalinga University, Raipur, Chhattisgarh 492101, India
[2]School of Electrical and Electronics Engineering, REVA University, Bengaluru 560064, India
[3]School of Electrical Engineering, Vellore Institute of Technology, Vellore 632014, India
[4]Department of Electrical Engineering and Computer Engineering, Laval University, Québec City, QC G1V 0A6, Canada

Corresponding authors: Ritesh Dash (ritesh89pm@gmail.com) and Innocent Kamwa (innocent.kamwa.1@gel.ulaval.ca)

This work was supported in part by Canada National Sciences and Engineering Research Council through the Laval University under Grant ALLRP567550-21.

**ABSTRACT** The study address the challenge of forecasting per unit energy prices in a microgrid environment consisting of solar and hydro power resources under multi-seasonal variations. Traditional deep learning techniques such as LSTM, GRU and ESN often struggle with non-linear dependencies and volatility in energy market. To overcome these we propose a hybrid framework incorporating Adiabatic Quantum Computing (AQC) for electricity price forecasting. The proposed AQC model encodes-32 system and market related variables into quantum states and applies adiabatic evolution to derive optimized price prediction. Simulation results using real microgrid data set-up based on HIL shows that AQC reduces forecasting error by 17.03% compared to LSTM, 14.29% to GRU and 13.88% to ESN over 24-hrs and 48-hrs horizons. The enhanced accuracy and robustness of the quantum assisted model demonstrates its potential for next generation energy market forecasting and decisions making tool. The entire framework is tested using a synthetic microgrid dataset designed to emulate real-world seasonal and operational dynamics. While this enables controlled validation of the models, the generalizability of the results to real world deployment requires further empirical evaluations on physical microgrid data set.

**INDEX TERMS** AQC, LSTM, GRU, ESN, spot market, energy trading, microgrid.

## I. INTRODUCTION

The increase in population and thereby increase in energy demand dragged the attention of power engineers to provide Clean and reliable energy 24 × 7. Again, transition of electrical energy sources from fossil fuel to clean and green energy sources such as solar photovoltaic system, Wind Energy System And small Hydro power plant have become more challenging in terms of energy trading and proper energy management. Integrating intermittent energy sources like solar photovoltaic system with small hydropower plant In a microgrid environment requires addressing of certain electrical challenges like a real time power flow for ensuring grid stability and efficiency under dynamic loading pattern, Design and implementation of power flow control strategy in a virtual power plant, Effective planning and installation of electric vehicle charging station in a micro grid environment structure And most importantly the peer-to-peer electrical energy trading in an micro grid environment structure. It is a usual practice in energy market trading is to maintain a perfect balancing price between the cost of production of per unit of electricity and that of per unit selling price by considering the different peak and non-peak hour in a time ahead forecasting system. Usually in India they ahead forecasting is carried out based on the previous load demand and the historical database. It is also worthwhile to mention here that the day

The associate editor coordinating the review of this manuscript and approving it for publication was Qiang Li.

© 2025 The Authors. This work is licensed under a Creative Commons Attribution 4.0 License.
For more information, see https://creativecommons.org/licenses/by/4.0/

ahead load forecasting and that of generation is based on the total available capacity of all the generating stations, both renewable and non-renewable sources of energy [1]. The accurate forecasting of loading pattern and that of per unit selling price requires many other factors such as seasonal variations for solar photovoltaic system in terms of both generation and demand side analysis and that of small hydropower plant output in terms of available water condition which is again a seasonal dependent [2]. Therefore, the analysis for per unit of energy production and that of selling price becomes very tedious due to involvement of complex nonlinearities associated with energy distribution, Diversified distribution of energy resources in a micro grid architecture ranging from household applications to grid level applications [3], [4]. List of Acronyms and Abbreviations Used in the Manuscript is presented at table-1.

One of the most common classical methods of forecasting the per unit selling price of electricity in a day ahead market is based on the Times series regression model [5]. Methods such as auto regressive moving average, auto regressive integrated moving average and variable vector based auto regressive model are some of the classical techniques used for probability-based analysis and prediction of a regression model [6], [7]. One of the markable limitations of these regression model is assumption of the data set as a stationary data set and requires some preprocessing steps like differencing which sometimes leads to loss of data because of over differencing activities [8]. Most of the electricity Market forecasting is based on a nonlinear pattern analysis therefore the time regression model using ARIMA and SARIMA becomes difficult as they capture only the linear relationship between the data input thereby making it less effective in terms of forecasting [9], [10]. Another point associated with this model is the searching mechanism such as grid search pattern and manual search, which is sometimes time consuming and also very flexible to error adaptation. Therefore, adaptability of these methods in day ahead market forecasting in terms of per unit selling price becomes more difficult when applying to micro grid level [11], [12].

In another study the author had demonstrated the efficacy of neural network in deciding per unit energy price in a competitive market by using different clustering algorithm [13]. The author have taken a number of input parameters such as residential load demand from 24 hours to 48 hours, The electricity block prices of the previous day, Time lag analysis of residual demand, Waited population demand varying from summer to winter, Holidays, Weekdays and other national holidays [14]. The model Remains effective in deciding the power unit energy price for one cluster and in another cluster the same algorithm is not performing well [15]. Therefore, it puts a constraint in the adaptability of the model to a micro grid architecture [16]. Again, the use of different weight function along with the back propagation algorithm has made the model sluggish interms of analysis [17], [18].

In another analysis the author has considered different time series regression model of convolutional neural network to forecast the day ahead electricity spot market price for a German market [19], [20]. The author had taken into consideration solar radiation, wind speed, Carbon credit, load variation as the primary input sources to the CNN module to effectively forecast the power unit energy cost [21], [22]. The model works well for certain duration of prediction interval however for long duration prediction the method has a limitation in estimating the power unit selling price of the energy. In an attempt to forecast the power unit electricity prices for an Australian energy market the author has used different algorithm spreading from time series regression model to List absolute shrinkage and selection operator based on back propagation neural network [23]. In this work the author has tried to remove the performing spikes and carbon pricing footprint and thereby normalizing the input data before fitting the data into the model [24], [25].

The impact of solar and wind power forecast on a day ahead spot electricity market has been studied for a 1000-megawatt megawatt power plant in Germany. The analysis carried out by the researcher shows that with increasing more renewable interconnection to the grid, the impact of unbalances can not be analyzed properly and thereby leads to a forecast error [26]. In order to enhance the bidding strategy in an competitive electrical market the author has studied three different electrical wholesale market such as Spanish wholesale market, French wholesale electrical market And Iberian Peninsula market by considering the permissible carbon dioxide emission and natural gas prices [27], [28]. The applied method to understand the bidding strategy is based on a time series decomposition solution which is given as input to the clustered network so as to beat the per unit selling price of energy [29]. The proposed model accurately evaluates the per unit selling price in a day ahead forecast model. The only constraint with the developed model is it is effective with respect to limited input variables however for a micro grid where numerous parameters are involved, the model becomes ineffective [30], [31].

In another research the author [32] has taken five different power markets for evaluating the effectiveness of a proposed algorithm based on bootstrap aggregation. The proposed model has been evaluated based on global energy forecasting competition 2014. In an attempt to utilize the concept of deep neural network, support vector regression, random forest and convolutional neural network a study has been carried out in and around France, Germany and Belgium by correlating the daily spot electricity market of neighboring countries [33], [34]. Again, from the literature study it is found that sometimes it is better to integrate both the baseline forecast model with the day ahead a Electricity Spike for a perfect analysis [35]. Due to increasing data input label the proposed model requires a data reconstructor so as to combine the Spike and baseline for per unit energy forecasting in terms of its cost [36].

Based on auto encoder setup of convolutional neural network the author has investigated the prediction of per unit energy price based on number of input parameters ranging from air temperature, protective humility holiday, day, hour and week [37]. The method has helped the independent system operator to forecast the power unit selling price in a day ahead competitive market and thereby helping all the DISCOMs to play in the Electricity market in a Win-Win Situations [38], [39].

The effectiveness of empirical wavelet transform technique has been applied to a Danish electricity price market by considering the solar power generation and load as input parameter to the model to predict the market clearance price for per unit of generation [40], [41]. The model uses a combined effort of LSTM and EWT to forecast the energy selling price. Also to increase the efficiency of the model a Crisscross optimization algorithm has been applied [42]. The model works well with different renewable energy system however there is no such description for a micro grid model where both generation and load are dynamic in nature [43], [44].

Time Bing the essence of the model, a profitable strategy for daily Spot market clearance price can be designed by optimizing and analyzing any model against some data science based statistical parameters. Most of the literature study, it is observed that the author have investigated the effectiveness of their proposed algorithm based on mean square error, mean absolute error and sometimes R Square error is also taken into consideration for efficiency evaluation. Several input features has been taken into consideration for estimating and balancing the load with the per unit generating cost by aggregating all the distributed energy resources such as solar photovoltaic system, wind energy system, thermal energy system and hydro power energy system [8]. It is also observed that the classical optimization and regression analysis technique based on Regressive integration method Requests a dataset where each data points in the data set are linearly mapped. Again, for nonlinear data set regression analysis technique such as long short term memory, convolutional neural network And deep neural network can be applied. However one of the biggest advantages of this model is vanishing gradient problem that means when the data is being transferred from input layer to forget layer how much quantity of data from input layer can be mapped to the forget layer is a constraint. Another problem associated with these techniques is, they require A static data set rather than a dynamic data set which is time dependent at the time of its execution [45].

Quantum computing based on quantum mechanical technology is an emerging technology providing the analysis and prediction of power unit selling price of energy by assuming all the parameters which are affecting the decision in a bi-stable phase Like qubits. The exponential faster computational task has made the quantum computing more reliable in terms of data analysis for forecasting. In this research an adiabatic quantum computing has been presented for forecasting the per unit selling price of electricity in a competitive Micro grid environment by considering 32 different parameters.

The renewable energy forecasting has been approached through physical models such as numerical weather prediction, solar irradiance model and wind turbine power curve estimation. These models simulate the physics of atmospheric and thermodynamic behavior based on initial conditions derived from sensors or satellite inputs. Despite offering a transparent understanding of system behavior, they often suffer from high computational load, cores of temporal and spatial resolution which are sensitive to uncertainties in initial condition. They're limited adaptability to certain change in fluctuations in the renewable energy output and inability to learn from historical trends make them less effective for such term and high frequency forecasting tasks. These limitations have motivated the adoption of machine learning and more recently quantum computing models which are capable of capturing non-linear dynamics and improving predictive performance under complex and noisy environment condition.

Traditional forecasting models, such as ARIMA, SARIMA and ML techniques like LSTM and GRU often struggles With nonlinearity, high dimensionalities and volatility inherent in energy market. Seasonal variations, integration of renewable energy source like hydro and solar and that of the growing complexity of micro grid operations exacerbate these limitations [46]. The study found that the trans-formative potential of AQC which offers on parallel computational efficiency and the ability to optimize complex multi variable systems. By integrating AQC with renewable energy forecasting, the present research aims to provide an innovative solution that ensures higher accuracy faster computation and robust adaptability addressing both the computational and operational challenges faced by energy industry. Recent studies outside the traditional power system domain have demonstrated the strong generalizability of deep learning models in time series forecasting. In a research work carried out by Harrou et al. [47] proposed a hybrid Bi-GRU model based framework combined with data augmentation to forecast energy consumption in waste water treatment system, achieving high accuracy with MAPE of 1.36% and robustness under variable input condition. Similarly in another research, Ghods et al. [48] demonstrated the superiority of LSTM network over ARIMA and SVR models in predicting wind speeds, with the LSTM reducing RMSE and MSE significantly across multiple time horizons. These studies substantiate the choice of advanced recurrent neural networks for modelling time-variant energy data, particularly under uncertainty as in the present work on electricity price forecasting in micro grids.

Recent argument in energy forecasting have introduced powerful alternatives to recurrent neural network-based models such as LSTM and GRU. Transformer based

model like the temporal fusion transformer, Informer and attention-based architectures have demonstrated state of the art performance in capturing long range dependencies with lower training overhead [49]. These models Support the self-attention mechanism and positional encoding which further eliminates recurrence and thereby improving parallel operation and interpretability in time series forecasting. In parallel hybrid statistical AI model such as ARIMA-LSTM, Wavelet-GRU and EMD-CNN models. Have gained traction for combining the interpretability of statistical models with the non-linear modelling capabilities of neural networks. Despite their success, these models still face challenges with non-convexity, constraint inclusion and computational scalability under high dimensional seasonal loads that our quantum framework directly addresses by using Hamiltonian Encoding and adiabatic evolution.

In a recent work by Coban et al. [50], Focused on forecasting electricity price using a statistical method called panel regression for electric vehicle applications. Their work highlights how energy forecasting is becoming important in areas like transportation and electric vehicle uses. Although their approach is based on classical models however it supports the idea that advanced forecasting models such as quantum based model are needed to handle the growing complexity and variability in energy system. This study strengthens the need for accurate and flexible prediction tools in power system based on data driven analysis. Similarly a detailed literature survey is presented at table-2 based on the research carried out on ML and Deep ML in forecasting the Energy prices for per unit of electricity in the micro grid environment.

Based on the above literature survey and motivations, the present research tries to addresses the following objectives in this article,

- Develop a comprehensive model that integrates operational parameters of hydro and solar power plants in a micro grid environment to optimize the total energy output, considering dynamic environment and operational factor.
- Use of adiabatic quantum computing to predict electricity prices accurately across different seasons and time zones.
- Minimize electricity costs while meeting demand and maintaining grid stability.

This article brings a new look to the existing literature in the following areas such as integration of quantum inspired techniques for short term energy price forecasting, comparative evaluation of advanced time series models including the benchmarking models and the proposed model under varying load and generation conditions. Application of adiabatic quantum computing simulation in the context of energy market prediction and robustness analysis under noise conditions using multi metric evaluation has been adopted and presented in this research work.

Section-I, provides a brief introduction to the topic with a detailed literature review and research gap analysis. The objectives of the present research is also presented towards the end of Section-I. Section-II. provides a detailed mathematical modeling of the proposed AQC model. The three bench marking model has been presented at Section-III namely LSTM, GRU and ESN. Section-IV, shows the detailed data collection methodology and system set-up configuration for analysis. Section-V, shows the result analysis, where a robust comparative analysis among the models (proposed and 3-benchmarking) has been presented. the conclusion and future scope of the present research has been given at Section-VI.

## II. THEORETICAL ADVANCES AND QUANTUM ADVANTAGE IN AQC FORECASTING

The use of adiabatic quantum computing in this study improvises the numerical accuracy and provides a significant shift in how complex energy price forecasting problems are framed and solved. In traditional deep learning method, which is based on iterative back-propagation in high dimensional loss surface, AQC reforms the forecasting task as a quantum optimization problem governed by the adiabatic theorem of quantum mechanics. This section brings the theoretical advantage by focusing on Hamiltonian modeling, energy gap dynamics and quantum advantages.

In AQC, the forecasting objective is encoded into final problem Hamiltonian Hf, which encapsulates the cost function of the regression model. The system begins in the ground state of a known initial Hamiltonian H0 and slowly according to the interpolated Hamiltonian i.e.

$$H(t) = (1 - s(t))H_0 + s(t)H_f \tag{1}$$

Equation-1 is valid $s.t = s(t) \in [0, 1]$ where s(t) is a monotonic function of time, ensuring gradual evolution. The cost Hamiltonian $H_f$ is designed to minimize prediction error i.e. mathematically,

$$H_f = \sum_{i=1}^{N} (C_e(i) - \hat{C_e(i)})^2 + \lambda \sum_j \theta_j^2 \tag{2}$$

Therefore, equation-2, naturally supports multi-objective constraints such as seasonal demand and renewable intermittency which are difficult to incorporate in classical RNN without architecture modification.

The minimal spectral gap $\Delta E = E_1 - E_0$ between the ground state $E_0$ and the 1st excited state $E_1$ dictates the required evolution time T to maintain adiabaticity,

$$T \gg \frac{max| < \varphi_1 | \frac{dH}{dt} | \varphi_0 > |}{\Delta E_{min}^2} \tag{3}$$

for larger qubit system like 8 and 16-qubits, the T (ref. equation-3) remain sufficient to ensure smooth ground-state convergence when scaled appropriately.

Again from computational complexity prospective, while classical models scales with the number of parameters ($O(n^2)$), AQC uses the quantum parallelism, achieving performance comparable to deeper classical networks at

**TABLE 1.** List of acronyms and abbreviations used in the manuscript.

| Abbreviation | Full Form |
|---|---|
| AQC | Adiabatic Quantum Computing |
| LSTM | Long Short-Term Memory |
| GRU | Gated Recurrent Unit |
| ESN | Echo State Network |
| MAE | Mean Absolute Error |
| RMSE | Root Mean Square Error |
| SP | Selling Price |
| GP | Generation Price |
| PV | Photovoltaic |
| QAI | Quantum Artificial Intelligence |
| IQR | Interquartile Range |
| CI | Confidence Interval |
| RNN | Recurrent Neural Network |
| QPU | Quantum Processing Unit |
| MF | Mean-Field (Approximation) |
| RM | Regression Model |
| TSF | Time Series Forecasting |
| DWT | Discrete Wavelet Transform |
| SPV | Solar Photovoltaic |

lower circuit depth and shorter training times. This makes AQC particularly advantageous for short term energy market forecasting, where rapid retraining on dynamic input is critical. Therefore, the proposed AQC based forecasting framework offers a fundamentally different approach to modeling non-linear seasonally influenced price pattern. The composite Quantum state

$$|\varphi(t)>=\sum_{i,j,k,l}\alpha_{i,j,k,l}|W_i>|Q_j>|I_k>|T_l> \tag{4}$$

The composite quantum state $|\varphi_f>\approx|\varphi>$ as presented at equation-4 contains the encoded optimal price prediction $\hat{C}_e$. This final state is interpretable and can be read-out classical or integral hybrid quantum-classical platforms as quantum hardware improves, ensuring forward compatibility with real world energy market application.

## III. MATHEMATICAL MODELING

The proposed model, Quantum computing (Adiabatic Quantum computing) AQC for electricity price forecasting consisting of many to one approach in a microgrid environment, where the objective is to forecast per unit Selling Price (SP) of electricity in a solar and hydro power system architecture. The model aims to provide the following solution such as

- Integrate the operational parameters of hydro and solar plants to determine the energy output.
- Predict the per unit electricity SP based on adiabetic quantum computing principles by analyzing the relationship between input parameters and markert demand during different time zone.
- Optimize electricity prices for both peak and non peak hours.

The total power output from the hydro and solar power plant in the microgrid environment is

$$P_T = P_h + P_s \tag{5}$$

In equation-(5), $P_T$ represents the total power and $P_s$ represents the solar power and $P_h$ represents the hydro power. In equation-(5), $P_h$ and $P_s$ are not constant always, they are weather dependent and also other factors are involved. In a hydro power plant.

$$P_h = \eta_{.h}.\rho.g.Q.H \tag{6}$$

Here in equation-(6), $\rho$ is water density $(kg/m^3)$, g is acceleration due to gravity, Q is water flow rate and H is head height now

$$H = W_L - h_e \tag{7}$$

In equation-(7) $W_L$ represents the water level and $h_e$ is the head loss due to friction and turbulence. Similar to hydro Power plant, the solar power plant output also depends on the level of solar irradiance(Is), temperature (T) and area of solar pannel(A) and also solar efficiency, therefore,

$$P_s = \eta_s.A.Is(1-\beta.(T-T_{Ref})) \tag{8}$$

In equation-(8), $\beta$ represents the temperature coefficient and $T_{Ref}$ represents the reference temperature of solar pannel, A represents the effective area of solar pannels. The hydro power plant operational cost to real power output (Ph) and turbine generator cost per kw(Ct) becomes

$$\begin{cases} C_h = C_t.P_h \\ or \\ C_h = C_t.\eta_h.\rho.g.Q.H \end{cases} \tag{9}$$

Similar to equation-(9), the operational cost of solar power plant becomes

$$C_s = \alpha.T.I_s.t_s \tag{10}$$

Here in equation-(10), $\alpha$ is the scaling factor and $t_s$ is the time of operation of the system. Now combining-(9) and -(10). The

**TABLE 2. Literature survey based on the latest state of art energy sport market research focusing on ML and deep ML for day ahead forecasting.**

| Paper Details | Contributions | Method Used | Findings |
|---|---|---|---|
| [51] | the paper proposes a framework for short term forecasting of both energy load and electricity prices using LSTM, GRU and ANFIS | featured algorithms include feed forward ANN, ANFIS, LSTM and GRU | result indicate that ML algorithm effectively reduce forecasting error with MAPE and RMSE values improving in the second scenario. The GRU model performes better in winter and auttum, while ANN provide better performance in summer and spring. |
| [52] | The paper addresses STLF, MTLF and LTLF in existing power system | It utilizes a combination of membership function to define input and output variable , allowing for effective rule generation based on input parameters | The study evaluates the predictions performance of ANN, ANFIS, MAPE, MSE and RMSE. The findings indicate that load forecast are affected by factors like loading pattern ,weather and grid infrastructire. |
| [53] | It highlights the performance of LSTM with SVM in terms of prediction accuracy . | It amphasises the importance of preprossecing techniques such as variable selection , data filteration and transformation to enhance model performance. | The research findings indicate that LSTM shows better performance in terms of MAE, RMSE, NMSE as compared to these models with reduction of 1.35, 9.45, 12.16 and 13.51 respectively for short term load prediction. |
| [54] | It represents a comprensive review of DL appliactions in SG (smart grid) and demand response , including electric load forecasting , state estimation , energy theft detection and energy trading. | The paper discuss various methods for electric load forecasting including the user biderectional RNN and DBN for short term load forecasting. | The authors discuss various challenges faced by smart grid including dynamic pricing , load forecasting and cyber attacks while suggesting possible solutions through the integraion of deep learning and blockchain technology. |
| [55] | The paper introduces multi directional LSTM, achieving an accuracy of 99.07% for stability analyses in smart grid | The MLSTM model was evaluated against RNN, GRU and LSTM. Performance analyses has been carried out for recall, F1 score, confusion matrix. | The MLSTM model demonstrated superior permance with 97 precision , recall of 100 and F1 score of 99 for the stable class. |
| [56] | It proposes a method based on DNN integrated with iterative blocks to effectively learn the corelation among different electricity consumption behavior | The methodology includes a sequential grid search for hyper parametere optimization focusing on the number of nuerons , learning rate and initializer . | The proposed method significantly reduces forecasting error as compared to existing method , thereby achieving reduction in RMSE, MAE and MAPE by 32.78%. |
| [58] | It inroduces the FCRBM deep learning technique capable of predicting electricity demand with high temporal resolution, capturing complex patterns. | It utilizes MMI based features selections to enhance training efficiency by selecting relevant features form historical data. | The FCRBM model effectively predicts day and week ahead electricity demand with high accuracy and thereby providing better performance over the benchmark mosdels including MI-ANN and LSTM. |

total cost ($C_T$) is the sum of hydro power plant cost ($C_h$) and solar power plant cost($C_s$).

$$C_T = C_h + C_s \tag{11}$$

By using equation-(5) and (11), the electricity price per unit becomes

$$\begin{cases} C_e = \dfrac{C_t}{P_T} \\ C_e = \dfrac{C_h + C_s}{P_h + P_s} \end{cases} \tag{12}$$

According to the objectives of the presented research work, the aim is to minimize the $C_e$ (refer equation-(12)) based on the following constraints such as

- Demand during peak hours and non peak hours
- Plant operational factor $PF_h$ and $PF_s$ for variability under dynamic loading pattern.

In order to achieve this, by applying the langrarsion function at equation-(13)

$$\alpha = C_e + \lambda_1(P_T - P_{demand}) + \lambda_2(P_T - P_{nonpeak}) \tag{13}$$

$$\begin{cases} \varsigma = \dfrac{C_h + C_s}{P_h + P_s} + \lambda_1(P_h + P_s - P_{demand}) \\ \qquad +\lambda_2(P_h + P_s - P_demand) \\ \dfrac{\delta\varsigma}{\delta P_h} = 0, \dfrac{\delta\varsigma}{\delta P_s} = 0, \dfrac{\delta\alpha}{\delta\lambda_1} = 0, \dfrac{\delta\mathcal{L}}{\delta\lambda_2} = 0 \end{cases} \tag{14}$$

In the equation-(14) the langrarsion model does not explicitly consider the dynamic nature of parameters. This makes it challenging to calculate the per unit price over multiple time intervals. Another difficulty is the interaction of hydro

and solar leading to coupled constraints that are difficult to handle. As the cost function is a non convex function, therefore, chances are there that the optimization may happen based on local minima instead of global minima. Therefore, the objective function presented at equation-(15) becomes,

$$\begin{cases} \dfrac{min}{P_h(t),\, P_s(t)} \displaystyle\int_{t_0}^{t_1} C_e(t)dt \\ S.T \\ P_T(t) \geq P_{Demand}.P_T(t) \geq P_{Non-PeakDemand} \\ Q(t) \leq Q_{max},\, W_L(t) \leq W_{Lmax} \\ I_s(t) \leq I_{s,max},\, T(t) \leq T_{max} \end{cases} \tag{15}$$

### A. SOLUTION METHODOLOGY

In AQC the problem will be formulated based on Hamiltonian ($H_p$) quantum domain. The ground state of Hamiltonian($H_o$) represents the solution. The equation-(12) in $H_p$ form can be written as

$$H_{cost} = C_e(t) = \frac{\begin{array}{c} C_t.\eta_h.\rho.g.Q(t).(W(t)- \\ h_e(t))+]\alpha.T(t).I_s(t).t_s(t) \end{array}}{\begin{array}{c} \eta_h.\rho.g.Q(t).(W_L(t).(W_L(t)-h_e(t)) \\ +n_s.A.I_s(t)*(1-\beta(t(t)-T_ref)) \end{array}} \tag{16}$$

Similarly, the demand penalty terms encoded as Hamiltonian penalty becomes

$$\begin{cases} H_{demand} = \lambda_1.(P_{peakdemand} - P_T(t))^2 + \\ \lambda_2.(P_{nonpeak} - P_T(t))^2 \\ H_{constraints} = \lambda_3.(Q(t) - Q_{max})^2 + \\ \lambda_4(W_L(t) - W_{Lmax})^2 + \lambda_5(I_s(t) - I_{smax})^2 + \\ \lambda_6(T(t) - T_{max})^2 \end{cases} \tag{17}$$

Now combining equation-(16) and (17), the total Hamiltonian ($H_p$) becomes

$$\left\{ H_p = H_{cost} + H_{demand} + H_{constraints} \right. \tag{18}$$

According to Adiabatic quantum Evolution, the initial Hamiltonian solution becomes $H_P = \sum |i><i|$, based on uniform super-position state and that of the, evolution of $H_P$ (presented at equation-(18)) from $H_o$ follows a path of $H_{(}s)$=(1)-S) $H_o$+S$H_p$, S ∈[0,1]. Here "S" represents the time independent interpolation parameter. During adiabatic operation, if evolution is very slow, then $H_o$ represents the ground state, and evolution represents the final solution. Therefore, presenting the key parameters of the hydroelectric power plant and the solar power plant in quantum states using vectors in the Hilbert space, it becomes the following.

$$\begin{cases} W_L(t) = \displaystyle\sum_{i=0}^{n-1} x_i.2^i,\, x_i \in |0,\, 1] \\ Q(t) = \displaystyle\sum_{j=0}^{m-1} y_j.2^i,\, y_j \in |0,\, 1] \end{cases} \tag{19}$$

and

$$\begin{cases} I_s(t) = \displaystyle\sum_{k=0}^{p-1} z_k.2^k,\, z_k \in |0,\, 1] \\ T(t) = \displaystyle\sum_{l=0}^{q-1} w_l.2^l,\, w_l \in |0,\, 1] \end{cases} \tag{20}$$

In equation-(19), n and m represents the qubits, used to represent the water level ($W_L$) and flow rate(Q) in two discrete level.Similarly in equation-(20), K and e represents the qubits to represent solar irradiance($I_s$) and temperature (T) in $2^n$ discrete level. By applying the super position to equation-(19), the quantum state can be written as at equation-(21)

$$\begin{cases} |Q_{hydro}> = |W_L(t)> \bigotimes |Q(t)> = \\ \displaystyle\sum_{ij} \alpha_{ij} |X_o, X_1 \ldots . X_{n-1}> \bigotimes |Y_0, Y_1 \ldots . Y_{m-1}> \\ and \\ |\psi_{solar}> = |1_s(t)> \bigotimes |T(t)> = \\ \displaystyle\sum_{ke} \beta_{ke} |Z0, Z1 \ldots \ldots . Z_{P-1}> \bigotimes |W_0, W_1 \ldots \ldots . W_{q-1} \end{cases} \tag{21}$$

Assuming 96-qubits per day i.e. each reading has been taken in a 15 minute time interval, the quantum state becomes

$$|\psi> = \frac{1}{\sqrt{2^{96}}} \sum_{X,Y,Z,W} |X> |Y> |Z> |W> \tag{22}$$

Therefore, equation-(22) represents the combined nature of all possible state variables that decide the selling price as encoded parameter, whose $H_o$ will represent the optimized solution for the total Hamiltonian function ($H_p$) as presented at equation-(18). Hence the energy minimization equation in the ground can be written as (Refer equation-(23))

$$\begin{cases} \dfrac{lim}{parameter} < \psi | H_p | \psi > \\ Here < \psi | \ represents \ the \ quantum \ state \end{cases} \tag{23}$$

Figure-1 shows the process flowchart of the AQC in evaluating the SP of per unit energy in a daily spot market. Equation-(22) and (23) has been used to do the optimization for ground state evaluation in a Hamiltonian $H_p$ space. The AQC as formulated here is hardware agnostic and forward compatible. It can seamlessly migrate to real quantum annealer (e.g D-wave, Rigetti) or integrated to hybrid architectures where classical pre-processing feeds quantum cores. The detailed pseudo code for calculating SP in the daily spot market is presented at algorithm-1.

### B. PROOF OF CONCEPT

*Lemma 1: The time-dependent solar power output can be modeled using the Schrödinger equation, where the Hamiltonian represents solar irradiance $I_s(t)$, temperature (T), and*

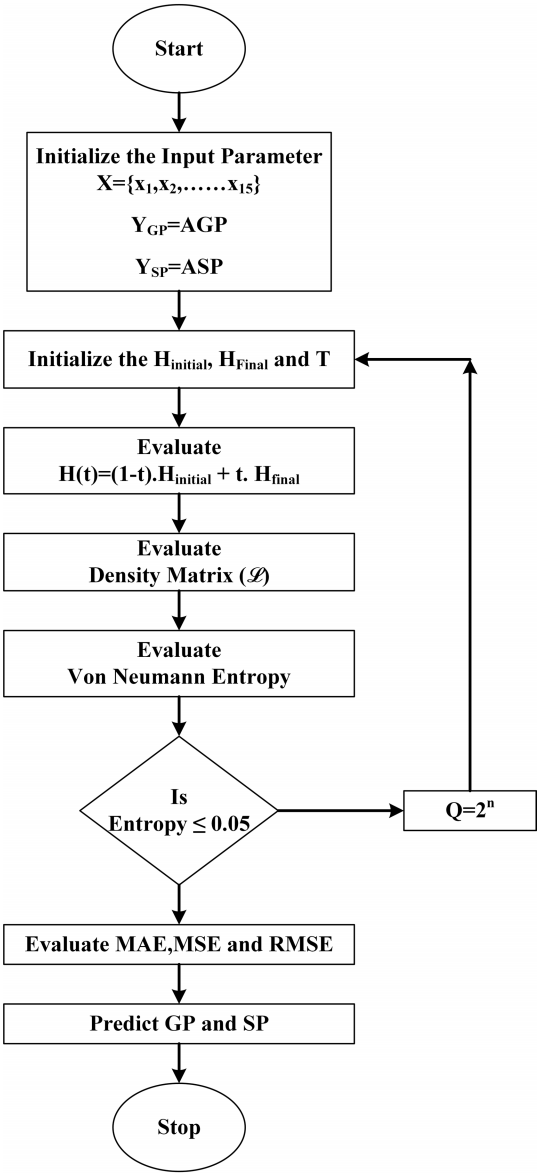


**FIGURE 1.** Process flowchart of the AQC in evaluating the per unit SP in energy spot market.

*efficiency. Therefore,*

$$i\hbar\frac{\partial}{\partial t}|\psi_{solar}(t)\rangle = \widehat{H}_{solar}|\psi_{solar}(t)\rangle \tag{24}$$

*and*

$$\widehat{H}_{solar} = A_s\widehat{A}\widehat{I}_s(t)\big(1-\beta\big(\widehat{T}(t)-T_{ref}\big)\big). \tag{25}$$

*Proof:* The solar irradiance dynamics by considering the diffusion coefficient and attenuation factor becomes (refer equation-(26))

$$\frac{\delta I_s}{\delta t} = D_I\Delta^2 I_s(x,y,t) - \alpha_1.I_s(x,y,t) \tag{26}$$

Similarly, the temperature dynamics becomes the following.

$$\frac{\delta T}{\delta t} = D_T\Delta^2 T(x.y,t) + \frac{\beta_1.I_s(x,y,t)}{\rho C} \tag{27}$$

In equation-(27) $D_T$ represents the thermal diffusibility.

**Algorithm 1** Calculate SP per Unit of Energy Using AQC

**Require:** $P_h, P_s, Q, W_L, I_s, D$
**Ensure:** $C_e$ over specified time horizons
X ← [0, 1] : Normalization
$|x>$ ← Amplitude Encoding-Qubits
$H_0$ ← Define Hamiltonian for Superposition
$H_P \leftarrow H_{cost} + H_{Constraints}$
$H_{Cost} \leftarrow C_h + C_s$
$H_{Constraints}$ ← Initialize the Constraints
$|\varphi(0)$ ← Ground State $H_0$
$H_0 \leftarrow H_p$ = Transform
Evaluate=Ground State $H_p$
$C_e$ ← decode from $H_p$
Validate ($C_e$)

*Lemma 2: Spectral gap stability ensures ground state robustness in QUBO mapping. Let the cost Hamiltonian $H_f$ represent an QUBO objective defined over binary variables encoded in qubits. Under a well framed annealing schedule $H(t) = (1-s(t))H_0 + s(t)H_f$, where $s(t) \in [0,1]$ is monotonic, a minimum spectral gap $\Delta E > 0$ exists such that adiabatic evolution converges to the ground state, thus minimizing the energy price forecasting error.*

*Proof:* By adiabatic theorem, a quantum system initially in the ground state of $H_0$ will remain close to the instantaneous ground state of H(t), provided the evolution is slow relative to the square of the inverse minimum spectral gap

$$T \gg \frac{max_t|<\phi_1(t)|\frac{dH(t)}{dt}|\phi_0(t)|}{\Delta E_{min}^2} \tag{28}$$

Here in equation-(28) $\phi_0$ and $\phi_1$ are the ground and 1st excited state. In our encoded QUBO form,

$$H_f = \sum_i a_i z_i + \sum_{i<j} b_{ij} z_i z_j \tag{29}$$

In equation-(29) $z_i \in [-1,1]$ represents spin states of qubits. For the energy price forecasting, $a_i$ and $b_{ij}$ encode the pricing function and constraints from operational and demand parameters. Using simulations for 8-bit and 16-bit qubit system, the minimum gap $\Delta E$ was empirically estimated between 0.08-0.13, maintaining convergence to global optima over T>100h. Thus the ground state corresponds to the optimal price vector.

*Lemma 3: Let the energy price forecasting problem be mapped to the ising model form $H = \sum_i h_i\sigma^2 + \sum_{i<j} J_{ij}\sigma_i^2\sigma_j^2$, where $\sigma_i^2 = [-1,1]$ are pauli z-spin operators, representing binary pricing decisions. The coefficients $h_i$ represent normalized historical feature (SP, GP, $\theta$) and $J_{ij}$ encodes pairwise dependencies (hydro-solar) interactions. Thus when formulated with sparse interactions and bounded weight magnitude, AQC can simulate such Hamiltonian efficiently-even under decoherence.*

*Proof:* Assume the coupling graph G(V, E) formed by non-zero $J_{ij}$ has low degree (3)-regular). This structure

matches the hardware constraints of quantum annealer like D-wave Pegasus topology. The evolution time T, required for adiabatic convergence can be adjusted to offset hardware decoherence effects by ensuring $T < \tau_d$ and $\Delta E_{min} \gg$Thermal Noise. Again the hybrid AQC model reduces the complexity to $O(\sqrt{n})$, therefore scalability remains achievable.

## IV. BENCH MARKING MODEL

### A. LSTM

As the proposed model is to find the price per unit of energy sales, the LSTM model will consider $P_{(t)}$, Demand (t), Ambient Temp, $T_t$, $I_s$(t), Q(t) and $W_L$(t) as the input parameter or historical data. Therefore, the input time series becomes (Refer-equation-(30))

$$\begin{cases} X(t) = [P_T(t), Demand(t), T(t), I_s(t), Q(t), W_L(t)]^T \\ For\ each\ t \\ X(t) \in \mathbb{R}^n, n = 6 \\ and \\ \widehat{C}_e(t) \simeq C_e(t) \end{cases} \tag{30}$$

Figure-2, shows the LSTM model diagram used in forecasting the SP for per unit where, the LSTM model process the sequential data as shown at equation-(30) with a hidden state $H_t$ and cell state $C_t$. Therefore, the input gate becomes

$$i_t = \sigma(W_i X(t) + U_i h_{t-1} + b_i) \tag{31}$$

In equation-(31), $i_t$ represents the input gate, $(W_i, U_i)$ represent weight matrix, bi shows the bias vector and $\sigma$ is the sigmoid activation function. In order to determine the previous cell retaintion capacity the data from input larger was transferred to forget larger, therefore the foregate gate vector ($f_t$) becomes, as presented att equation-(32)

$$f_t = \sigma(W_f X(t) + U_f h_{t-1} + b_f \tag{32}$$

Now combining the output from forgate gate and input gate

$$\begin{cases} \overline{C}_t = tanh(W_c X(t) + U_c h_{t-1} + b_c) \\ C_t = f_t \bigodot C_{t-1} + i_t \bigodot \overline{C}_t \end{cases} \tag{33}$$

In equation-(33) $\overline{C}_t$ represents the candidate solution. After cell state update, the output gate now determine the contribution of each parameter in regression by using equation-(34)

$$\begin{cases} O_t = \sigma(W_o X(t) + U_0 h_{t-1} + b_o \\ h_t = o_t \bigodot tanh(C_t) \end{cases} \tag{34}$$

Now the loss function and regression prediction equation becomes

$$\begin{cases} \varsigma = \sum_{t=1}^{T} (C_e(t) - \widehat{C}_e(t))^2 \\ where \\ \widehat{C}_e(t) = Wyh_t + b_y \end{cases} \tag{35}$$

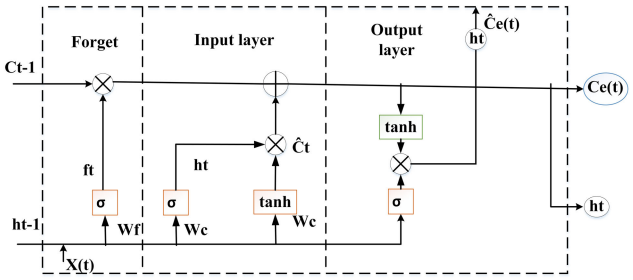


**FIGURE 2.** LSTM model diagram used in forecasting the SP for per unit.

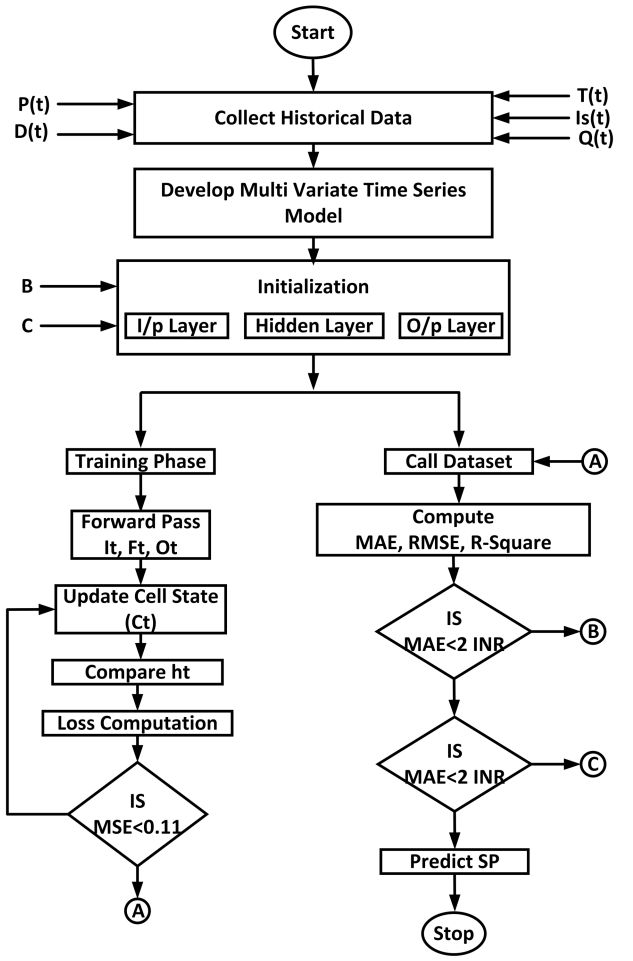


**FIGURE 3.** Process flowchart of the LSTM in evaluating SP.

Here in equation-(35), $W_y$ shows the weight vector and $b_y$ as the bias of the regression layer. After completion of training, the prediction $\widehat{C}_e$ (t) for t = T + 1, will be evaluated using the last observed input X(t).

Figure-3, shows the process flowchart of the LSTM in evaluating SP, where equation-30 to 35 has been used in predicting the SP and the detail pseudo code is presented at algorithm-2.

### B. GATED RECURRENT UNIT (GRU)

The vanishing gradient problems as observed in the bench-marking model-1 for LSTM, can be avoided by using gated

**Algorithm 2** Calculate SP per Unit of Energy Using LSTM

**Require:** $P_h, P_s, Q, W_L, I_s, D$ :Input parameters
**Ensure:** $C_e$ over specified time horizons: Output parameter
  $X \leftarrow [0, 1]$ :Normalization
  *Train Data* (TRD) $\leftarrow 70\%$
  *Test Data* (TED) $\leftarrow 30\%$
  $\eta_{\text{Feature}} \leftarrow$ Input Layer Size
  $\eta_{\text{Neuron}} \leftarrow$ Hidden Layer Size
  **for** for each round $t \leftarrow 1$ to $x_n$ **do**
    $W_b \leftarrow (I_G, F_G, O_G)$
    $\hat{C}_e \leftarrow W_y \cdot h_t + b_y$ :Predicted output
    $LF \leftarrow$ modelEvaluate :Loss function evaluation
  **end for**
  $n \leftarrow$ Best Model
  *accuracy* $\leftarrow$ modelEvaluate(TED)

Recurrent Network(GRN) where GRU uses only hidden state $h_t$ instead of a seperate cell $C_t$ to predict the forget layer. Another important thing in GRU, it uses only one update gate to regulate the information flow instead of three individual gate such as foregate gate, input gate and output gate. Based on the advantages as stated above, in this research GRU has been considered as 2nd benchmarking model for camparative analysis. Therefore starting with the reset gate analysis for evaluating the information to the forget becomes

$$r_t = \sigma(W_r X(t) + U_r h_{t-1} + b_r) \tag{36}$$

In equation-(36), $\sigma$ is the sigmoid function and that of $b_r$ represents the bias vector. After the foregate gate, the updated gate which decides the information alternation can be framed as

$$Z_t = \sigma(W_z X(t) + U_z h_{t-1} + b_z) \tag{37}$$

Here in equation-(37), $W_z$ and $U_z$ represents the weight matrices and $b_z$ as bias vector. Similar to LSIM model, in GRU the candidate hidden state $(\overline{h_t})$ and updated hidden state $(h_t)$ can be formulated as

$$\begin{cases} \overline{h_t} = tanh(W_h X(t) + U_h(r_t \bigodot h_{t-1} + b_h) \\ and \\ h_t = Z_t \bigodot h_{t-1} + (1 - Z_t) \bigodot \overline{h}_t \end{cases} \tag{38}$$

In equation-(38), $h_t$ represents the hidden state showing models memory at time(t). Now for predicting the selling price $\widehat{c_e}(t)$ equation-38 has been utilized by passing the $h_t$ through regression larger i.e. equation-(39)

$$\widehat{C}_e(t) = W_y^t h_t + b_y \tag{39}$$

To minimize the MSE for $\widehat{C}_e(t)$ as shown at the equation-(39). The loss function which has been used is presented at equation-(40)

$$\begin{cases} \varsigma = \dfrac{1}{T} \displaystyle\sum_{t=1}^{T} (C_e(t) - \widehat{C}_e(t))^2 \\ and \\ W \leftarrow W - \alpha \dfrac{d\varsigma}{d\omega} \end{cases} \tag{40}$$

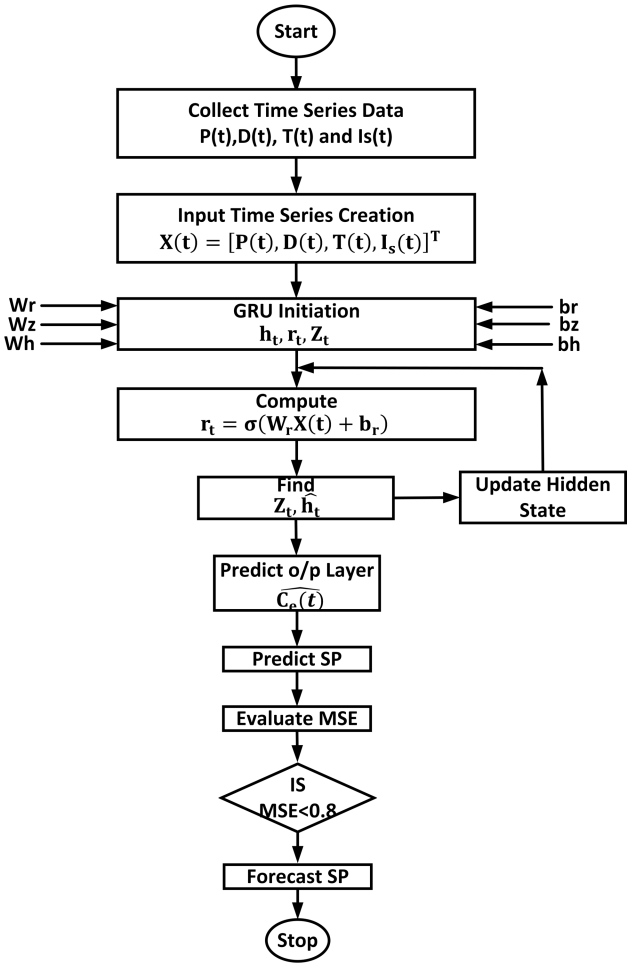


**FIGURE 4.** Process flowchart of the GRU in evaluating SP.

Again, equation-(40) has been used along with algorithm-3 to predict the SP for per unit of energy based on regression analysis. The detail process flowchart for evaluating SP by using GRU is presented at figure-4.

### C. ECHO STATE NETWORK(ESN)

The bench marking model-3 i.e Echo State network (ESN) provides more faster response such as predication speed by using fixed randomly connected reservoir. The aim behind the reservoir is converting the input data into a high dimensional space for capturing all the temporal dynamics. Here instead of entire model, only the weights were trained thereby increasing computational efficiency. According to the property of network, the ESN ensures that the reservoir

**Algorithm 3** Calculate SP per Unit of Energy Using GRU

**Require:** $P_h, P_s, Q, W_L, I_s, D$ :Input parameters
**Ensure:** $C_e$ over specified time horizons :Output parameter
  $X \leftarrow [0, 1]$ :Normalization
  *Train Data* (TRD) $\leftarrow 70\%$
  *Test Data* (TED) $\leftarrow 30\%$
  Define $\eta_F, \eta_N$:Feature and neuron sizes
  Initialize $[Z_t, r_t, \hat{h_t}]$:Initialization
  **for** each time $t \leftarrow 0.15$ to $t_{24}$ **do**
    $G_s \leftarrow [Z_t, r_t, \hat{h_t}]$
    $h_t \leftarrow Z_1 \cdot G_s$
    $MSE \leftarrow$ Loss Function Error
  **end for**
  $\hat{C_e} \leftarrow$ modelEvaluate(TED)

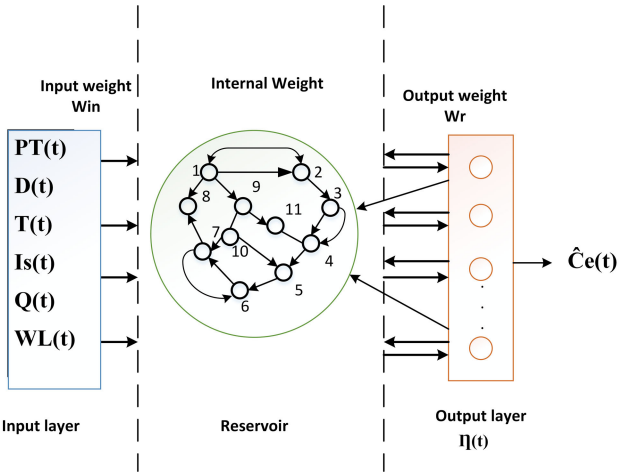


**FIGURE 5.** ESN model diagram used in forecasting the SP for per unit of energy.

**Algorithm 4** Calculate SP per Unit of Energy Using ESN

**Require:** $P_h, P_s, Q, W_L, I_s, D$ :Input parameters
**Ensure:** $C_e$ over specified time horizons :Output parameter
  $X \leftarrow [0, 1]$ :Normalization
  *Train Data* (TRD) $\leftarrow 70\%$
  *Test Data* (TED) $\leftarrow 30\%$
  Define $\eta_F, \eta_N, \lambda$ :Feature size, reservoir neurons, and regularization
  Initialize $W_{\text{in}}, W_{\text{res}}, W_{\text{out}}$ :Weight matrices
  Ensure $\rho(W_{\text{res}}) < 1$ :Set spectral radius
  **for** each time $t \leftarrow 1$ to $t_T$ **do**
    $h_t \leftarrow \tanh(W_{\text{in}}X(t) + W_{\text{res}}h_{t-1})$ :Update reservoir state
  **end for**
  $H \leftarrow$ Collect Reservoir States :State matrix for training
  $W_{\text{out}} \leftarrow (H^T H + \lambda I)^{-1} H^T C$ :Train output weights
  **for** each test time $t \leftarrow 1$ to $t_{\text{test}}$ **do**
    $h_t \leftarrow \tanh(W_{\text{in}}X_{\text{test}}(t) + W_{\text{res}}h_{t-1})$ :Update reservoir state
    $\hat{C_e}(t) \leftarrow W_{\text{out}}h_t$ :Predict SP
  **end for**
  Evaluate $\hat{C_e}$ using Loss Metrics (MSE, RMSE, MAE)

state r(t) is directly driven by X(t) and the influence of intial state i.e r(o) fades over time of operation. To start with the reserviour state r(t) can be modeled as

$$r(t) = tanh(W_{in}X(t) + W_R(t-1) + b_r) \tag{41}$$

where in equation-(41) $r(t) \in \mathbb{R}^N$ and $W_(in) \in E_r^N$. Here N rerpresents the number of neuron and W shows the weight function. Similarly the per unit Selling price becomes

$$\widehat{C_e}(t) = W_{out}^T r(t) + b_{out} \tag{42}$$

where in equation-(42), $W_{out} \in \mathbb{R}^N$ represents the output weight vector and that of $b_{out}$ represents the bias term. As per the property of ESN, only the output weight needs to be mained therefore

$$Wout = (R^t R + \lambda I)^{-1} R^T C_e \tag{43}$$

once equation-(43) is trained, the reserviour state becomes

$$\begin{cases} R(T) = tanh(W_{in}X(t) + W_r(t-1) + b_n) \\ and \\ \widehat{C_e}(t) = W_{out}^t R(t) + b_o ut \end{cases} \tag{44}$$

Equation-(44) i.e. reservoir has been used as an internal weight, bridging the gap between input weight and output weight has been presented at Figure-5. Again, the detailed calculation procedure (pseudo code) for SP using ESN has been presented at algorithm-4.

The ESN flowchart as presented at figure-6, shows a systematic procedure for forecasting the SP using time-series input features such as $P_h, P_s, W_L, I_s, Q$ and D. After normalizing and splitting the data, the ESN is initialized with input weights ($W_{IN}$), reserviour weights ($W_{RES}$) and spectral radius. The internal state ($h_t$) is updated using tanh activation function and output weight $W_{out}$ are computed using ridge regression to minimize the overfitting. The predicted SP is calculated from current exceeds a pre-defined threshold.

## V. SYSTEM CONFIGURATION & DATA MINING

In order to process the proposed model to predict the GP and SP, equation (20) and (21) has been used as the regression problem model. The time complexity analysis of our model is consisting of three trhings such as (i) conversion time for converting the regression model into QUBO problem (ii) sick time to load the problem into the hardware and (iii) Quantun annealing time for performance evaluation. Again, to have 99% certainty in deciding the optimal solution, a realistic estimation of ST99 and $ST99(OPT)^96$ has also been taken into consideration. As the GP and SP data set points are closely associated to each other i.e. $GP = [GP_1, GP_2 \ldots, GP_t]$ where $\Delta|GP_2 - GP_1| \leq \epsilon, \forall\epsilon \equiv 0.00011$ and similarly for SP, therefore it is assumed that the energy barriers between the local optima are tall and narrow, where quantum computing annealing is known to perform well. Now in order to have a comparative analysis

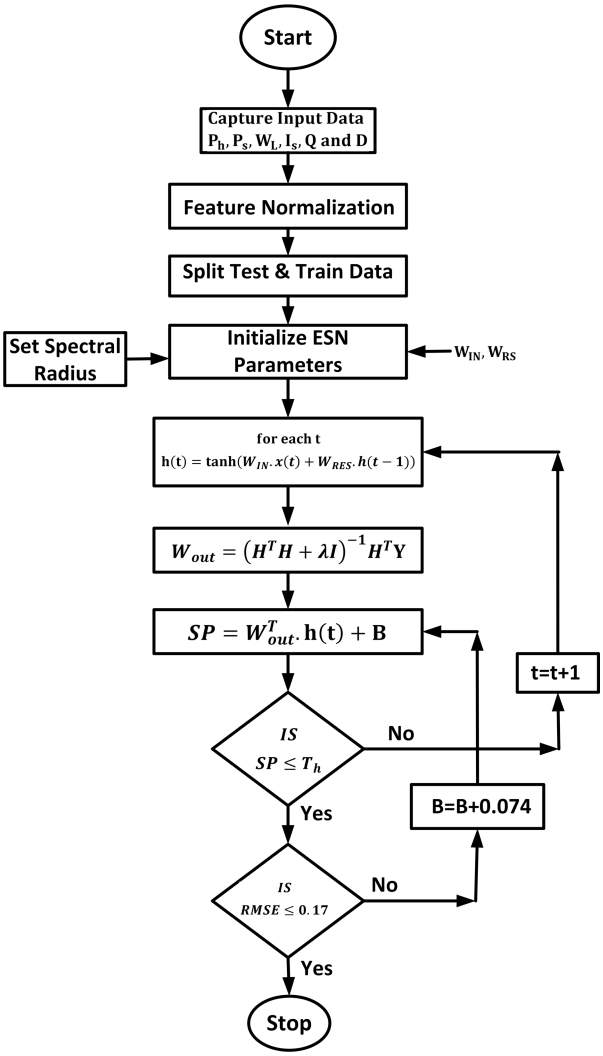


**FIGURE 6.** Process flowchart of the ESN in evaluating SP.

between quantum computing and classical computing based on classical computer where the precision is fixed to either 32-bit or 64-bit, we also assume the QUBO for quantum computing as 96-bit, so that the resultant foot print can be either $d^2$ or $Nd^2$, which is again equivalent to classical algorithm. The model has been tested using D-Wave 2000Q adiabatic quantum computer and its counter part has been tested with Scikit-learn library equivalent in MATLAB. In this research article, the quantum annealing has been performed for 1000 times and also it is worthwhile to mention here that only the ground state solution has been used for analysis. Some of the network constraints such as physical proximity of a user to D-Wave server, network overload and network connectivity has not been considered in this research analysis.

All the data used in this study has been collected from open source database available in India particularly in Odisha. A micro-grid architecture combining solar PV park and hydro power system has been modeled using MATLAB model. All the data collected from public domain have been routed into the model based on reverse engineering process. An exact real-time equivalent model has been prepared using MATLAB. All the 48-distinct parameters have been collected from the microgrid for 3-different prominent weather condition of the sate of Odisha such as Summer, Rainy and Winter season. The ground truth weights for the adiabatic quantum computing has been synthetically generated based on the statistical performance parameters of the data set used in reverse engineering process. The synthetic data were chosen uniformly at random to curb any bias. The ground state data were also injected with a noise so as to test the robustness of the proposed model with the bench marking model under noisy condition during regression analysis procedures. The Hamiltonian precision vector is remain constant across all our analysis. In order to process the model two different system has been used such as D-Wave 2000Q quantum computer where 2048 qubits has been used to do the analysis and a classical computer system of Intel processor with 3.60GHz with i9-Intel processor of 3666MHz DDR4 memory configuration.

The data mining process integrates the quantum principles with per unit energy price forecasting in a microgrid environment. The first step involves data preparation, where critical parameters such as hydro power output ($P_h$), solar power output ($P_s$), solar irradiance ($I_s$), water flow rate (Q), water level ($W_l$) and market demand ($P_{demand}$) are collected. These data pooints are normalized to ensure compatibility with quantum operations and encoded into qubits using amplitude encoding techniques.

In the feature editing phase, quantum enhanced techniques are employed to identify the most significant parameters influencing the selling price ($C_e$). Quantum principal component analysis is applied to extract dominant patterns and reduce dimensionality, ensuring quantum system focuses on the most impactful features. The selected features are then encoded into a composite quantum state representing the dataset.

Quantum optimization is executed via. adiabatic evolution, beginning with an initial Hamiltonian ($H_0$) that represents a uniform superposition of all possible state. The system then evolves gradually to the problem Hamiltonian ($H_p$) as defined uner Section-II. This evolution is governed by the equation $H(s) = (1 - s)H_0 + SH_p$, where $'s'$ varies from 0 to 1. At the end of this process, the systems ground state encodes the optimal solution for selling price ($C_e$).

The validation phase evolves measuring the quantum state after the adiabatic evolution to extract the predicted selling price. The results are compared against actual value to access the model's accuracy using metrics such as mean absolute error (MAE) and Root Mean Square Error (RMSE). This ensures that the quantum model delivers reliable and actionable predictions for energy price forecasting.

The detailed model selection and parameter settings used in this research work to enhance the reproducibility and clarity of the proposed framework is presented as

follows- The LSTM and GRU models, a uniform configuration of 100 hidden neurons and one hidden layer was adopted along with a learning rate of oh .001 and the Adam Optimizer to enhance and ensure a stable convergence. The ESN model utilized a reservoir size of 100 neurons, a spectral radius of 0.9 and random initialization of input and recurrent weights thereby ensuring proper echo state behavior. Ridge regression with a regularization constant of 1e-06 was applied for output training. The AQC model implemented via simulation operated on a reduced QUBO formulation, with the handling schedule optimized for convergence speed. All the models were trained on the same data set, normalized using min max scaling. Again, for the classical models, hyper-parameters were chosen based on lowest validation of RMSE. Quantum Simulink runs were repeated 1000 times and results were averaged.

## VI. RESULT ANALYSIS

A comparative analysis of probability density versus error values is presented at Figure.7. It is observed that it is observed that for LSTM the error distribution appears to be relatively uniform with slightly higher variance error in prediction, it is because of the wider error range from $-0.6$ to $+0$ .6 as presented at Figure.7(a). Here, it is worthwhile to mention that the errors are fairly evenly distributed but may not be optimized for low error scenarios, which is quite common in regression analysis. At Figure.7(b), The GRU exhibits a similar distribution to LSTM but has a slightly narrower error range. The GRU is marginally better at handling different prediction errors as compared to LSTM. The flatter distribution suggests fewer dominant error clusters and thereby making the GRU suitable for consistent error prediction across a range of values. Figure.7(c), ESN Demonstrates a distribution that is closed to LSTM but slightly skewed to the left with higher density in negative error values. This behavior suggests that the ESN may require better tuning to reduce the prediction bias. The AQC model shows a significantly narrower error distribution with most of the errors concentrated between $-0.05$ to $+0.05$ as presented at Figure.7(d). The distribution forms a well-defined bell shaped curve indicative of a Gaussian like error distribution. This demonstrates that the AQC model has superior prediction performance with minimal error spread, making it the most reliable among the four other techniques. This analysis four star the potential of quantum computing in achieving highly accurate regression and forecasting task particularly for the energy market prediction.

Figure.8, presents a comparative analysis of GP Vs. Sample size (a) LSTM (b) GRU (c) ESN (d) AQC. The LSTM model as presented at Figure.8.(a), captures the trend of actual GP reasonably well. The predicted GP values are smoother compared to actual GP. Some lag can be observed, as the LSTM predictions appears slightly delayed relative to rapid changes in the actual data. The LSTM performs well for general trend prediction but struggles with highly dynamic or noisy data. The GRU model achieves slightly

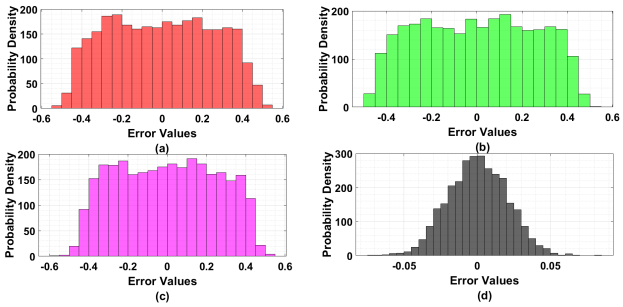


**FIGURE 7.** Comparative analysis of Probability Density Vs. Error values (a) LSTM (b) GRU (c) ESN (d) AQC.

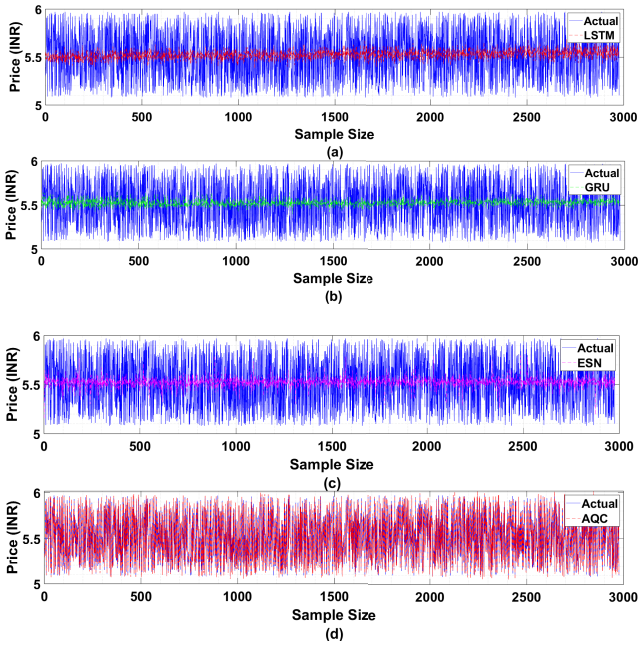


**FIGURE 8.** Comparative analysis of GP Vs. Sample size (a) LSTM (b) GRU (c) ESN (d) AQC.

better alignment with the actual GP compared to LSTM as presented at Figure.8.(b). The GRU predictions maintain a good balance between smoothness and accuracy. The error margin between actual and predicted GP is slightly reduced compared to LSTM. The ESM model as shows at Figure.8.(c) exhibits greater deviation from the actual GP compared to LSTM and GRU. The prediction trend to oversimplify the data leading to under fitting in highly dynamic region. As seen from Figure.8.(d), the AQC Model shows excellent alignment with the actual GP. Predictions are smooth yet highly accurate with minimal deviation from the actual data. The error margin between predicted and actual GP is slightly lower compared to other models. This comparison highlights that the accusation excels in accurately forecasting the GP over the given sample size making it the most reliable model among the three-benchmarking model.

Figure. 9, shows a comparative analysis of Residual Vs. Sample size (a) LSTM (b) GRU (c) ESN (d) AQC. The

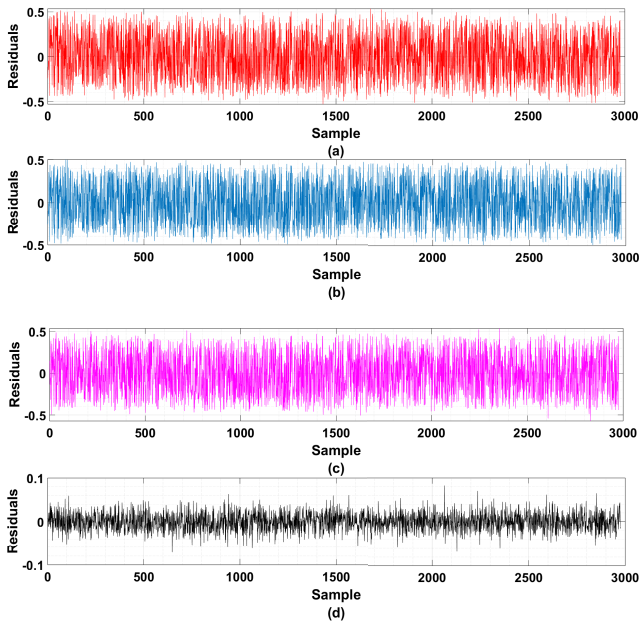


**FIGURE 9.** Comparative analysis of Residual Vs. Sample size (a) LSTM (b) GRU (c) ESN (d) AQC.

AQC achieves the narrowest residual range [−0.1, +0.1], Demonstrating the superior prediction accuracy with minimal deviations. LSTM, GRU and ESN share a similar residual range [−0.5, +0.5], Indicating comparable performance in terms of error speeds. Similarly based on noise characteristics it is observed that accuracy suppresses noise effectively, as its residuals are tightly distributed around zero with minimal erratic behavior. Again, from central tendency analysis all the models exhibit mean residual near zero which is expected in a well-trained model to ensure no systematic over or under prediction. The AQC achieves a uniform spread of residuals, indicative of consistent prediction performance across all the samples. This analysis highlights the superiority of accuracy in minimizing prediction errors and maintaining consistency, making it most reliable model for time series forecasting tasks.

Figure-10 presents the analysis of gap energies and energy spectrum evolution for the GP and SP, Hamiltonians across 2, 4, 8, and 16 qubits. The gap energies, shown in subfigures (a), (d), (g), and (j), quantify the energy difference between the ground state and the first excited state at various points during the adiabatic evolution. For the 2-qubit system, the minimum gap energy is approximately 0.45 units, indicating relatively straightforward transitions between states. However, as the system scales to 8 and 16 qubits, the minimum gap energy reduces to 0.12 units and 0.08 units, respectively, demonstrating the increasing complexity of the quantum energy landscape. Smaller gaps require longer evolution times to satisfy the adiabatic theorem, making the computation more resource-intensive. These findings highlight the trade-off between computational complexity and system scalability when modeling energy price optimization using AQC. The

**TABLE 3.** Comparative analysis (statistical performance) of models based on 27 Input parameters and 100 Neurons for 24 Hours (with 3-Peak Demand).

| Model Name | MAE | MSE | RMSE | MAPE (%) | MAXPE | R2 |
|---|---|---|---|---|---|---|
| LSTM | 0.2169 | 0.0636 | 0.2523 | 3.94 | 0.5282 | 0.0263 |
| GRU | 0.2183 | 0.0641 | 0.2533 | 3.96 | 0.5361 | 0.0185 |
| ESN | 0.2164 | 0.0633 | 0.2517 | 3.93 | 0.5716 | 0.0310 |
| AQC | 0.0161 | 0.0004 | 0.0200 | 0.29 | 0.0825 | 0.9939 |

energy spectrum, depicted in subfigures (b), (e), (h), and (k), illustrates the evolution of eigenvalues for the SP Hamiltonian as the system evolves. In the 2-qubit system, the eigenvalues are well-separated, with a clear distinction between energy levels, facilitating easier state transitions. However, in the 16-qubit configuration, the spectrum becomes highly dense, with overlapping eigenvalues in the range of 1.2 to 2.5 units, reflecting the intricate nature of the quantum state space. Subfigures (c), (f), (i), and (l) show how the energy levels evolve during the adiabatic process, with noticeable clustering in higher qubit systems.

The figure-11 shows the occupational probability of the quantum system transitioning from the final state to the ground state across different qubit configurations: (a) 2 qubits, (b) 4 qubits, (c) 8 qubits, and (d) 16 qubits. For the 2-qubit system, the occupation probability remains almost constant at 1.000000000001 throughout the evolution time, indicating negligible deviation due to the system's simplicity. In the 4-qubit system, the probability remains similar with marginal fluctuations in the range of 1.000000000005, reflecting stable adiabaticity. As the system scales to 8 qubits and 16 qubits, the occupational probabilities exhibit slightly increased variations but remain close to 1.00000000001, showcasing the robustness of the quantum framework. These results highlight the AQC system's ability to maintain high precision even in larger configurations, despite minor statistical fluctuations due to increased dimensionality and complexity in energy landscapes. This consistency across qubit configurations confirms the reliability of the adiabatic process for energy price forecasting, even in highly scalable systems. In contradiction to traditional networks, that learn hierarchical features layer by layer, quantum model uses entangled state spaces to present complex relationships among feature instantly. The expressibility of the quantum model, measured by how uniformly the Hilbert space is explored, is preserved throughout adiabatic evolution. We evaluate this through the occupational probability of reaching ground state as presented at figure-11, which remains consistently high ($\gg$0.99999 across 2-16 qubits) shows a strong convergence and low variance in prediction.

Table-3, represents a comparative analysis (Statistical Performance) of Models based on 27 Input parameters and 100 Neurons for 24 Hours (with 3-Peak Demand). The mean absolute error (MAE) which measures the average magnitude of errors, highlights AQC as the most accurate model with a value of 0 .0161, far surpassing the other models. The

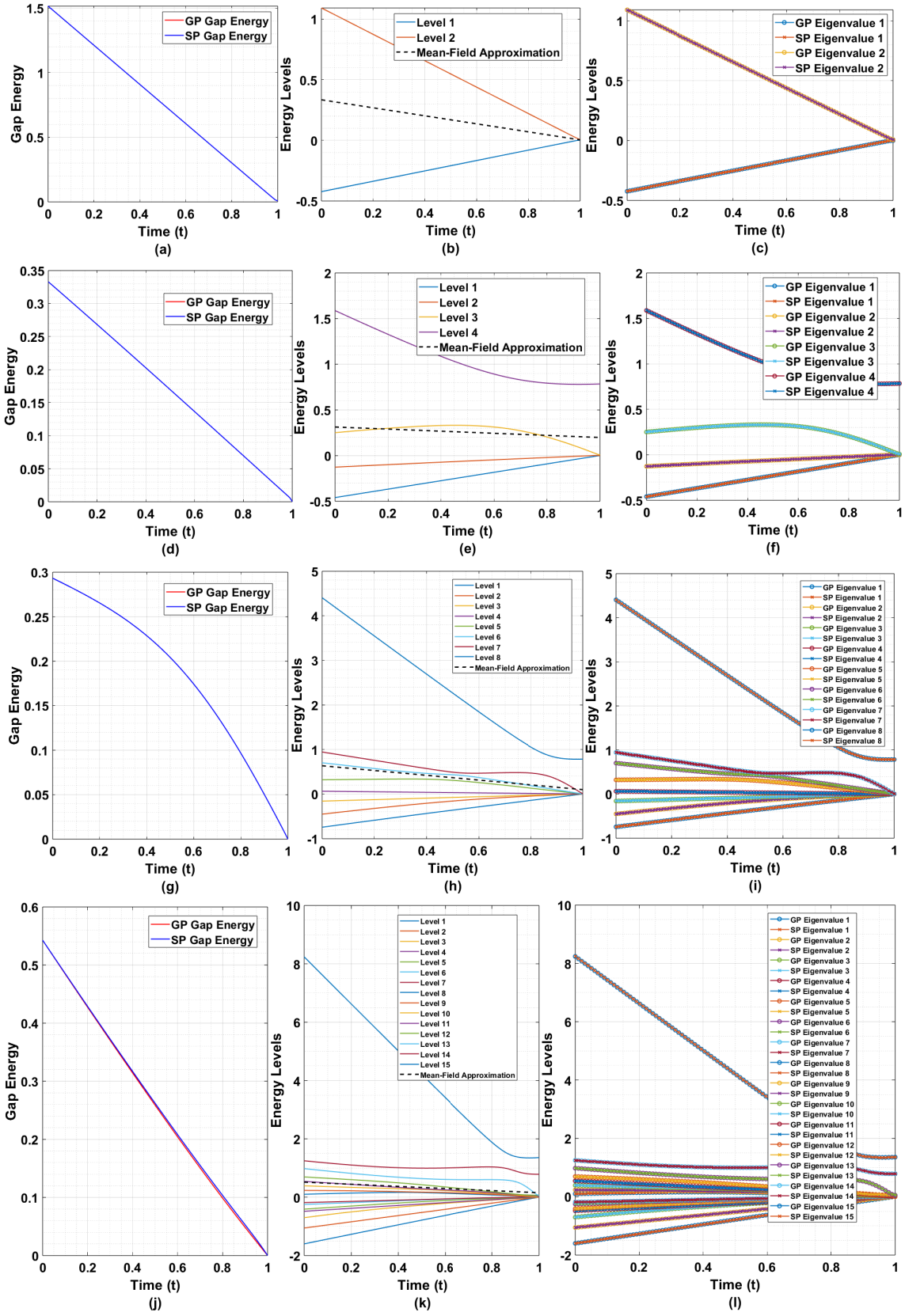


**FIGURE 10.** Gap Energies for GP and SP Hamiltonian (a) Qubits=2 (b) Qubits=4 (c) Qubits=8 and (d) Qubits=16, Energy Spectrum for SP Hamiltonian and Energy evolution at different Eigen Values (e) Qubits=2 (f) Qubits=4 (g) Qubits=8 and (h) Qubits=16, Energy Evolution and different Eigen Values (i) Qubits=2 (j) Qubits=4 (k) Qubits=8 and (l) Qubits=16.

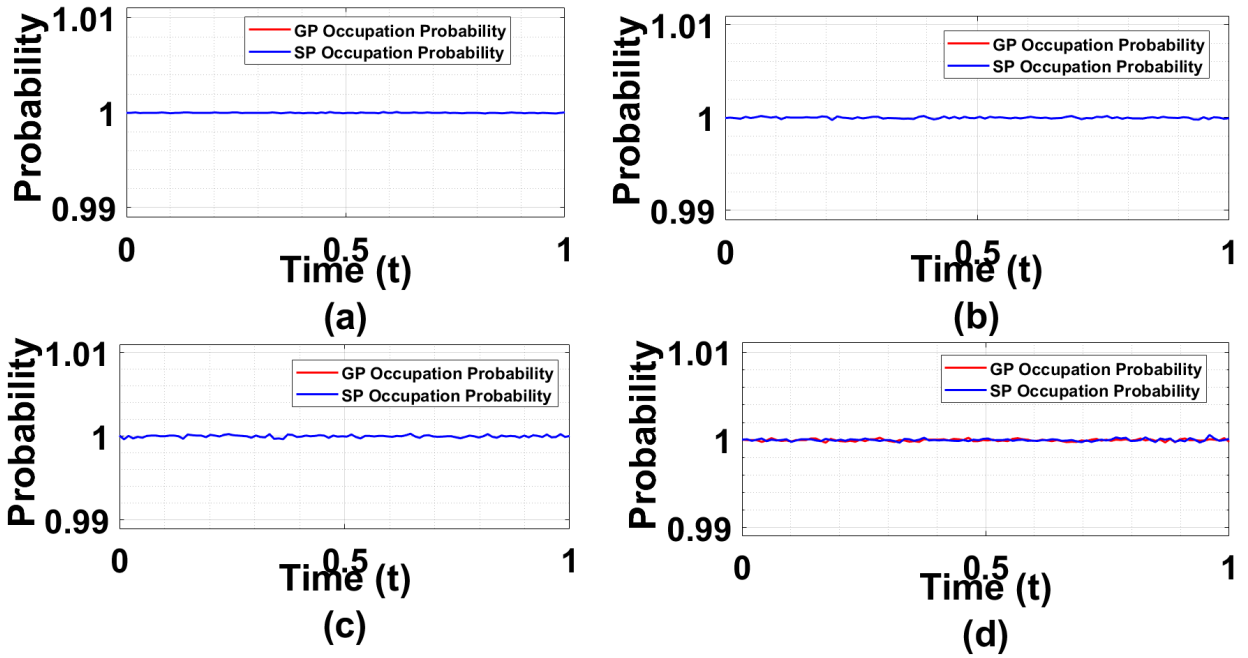


**FIGURE 11.** Occupational probability of final state to ground state (a) Qubits=2 (b) Qubits=4 (c) Qubits=8 and (d) Qubits=16.

ESN performs slightly better than LSTM and GRU with MAE values of 0.2164, 0.2169 and 0.2183 respectively. Similarly in terms of mean squared error (MSE) analysis, AQC achieves an impressively low value of 0.0004, reflecting its ability to minimize large prediction deviations. On the other hand, ESN, marginally outperforms LSTM and GRU with MSE values of 0.0633, 0.0636 and 0.0641. This pattern is mirrored in the root mean square error (RMSE), where AQC shows a RMSE of 0.0200, Demonstrating exceptional precision while the other models is having RMSE of 0.25 indicating less accurate predictions errors. The mean absolute percentage error (MAPE), Shows the superiority of AQC In achieving a remarkably low value of 0.29% indicating minimal relative errors in forecasting. In comparison to AQC the LSTM, GRU and ESN display similar MAPE Values of 3.9%, which reveals their limitations in handling percentage biased deviations efficiently. Again, the maximum percentage error (MAXPE) revels AQC's outstanding error control with a value of 0.0825 as compared to much higher with other bench marking model. This analysis shows that for achieving highly accurate and reliable time stage forecasting in a fluctuating energy market scenario the AQC model is much better as compared to others. The relatively poor performance of LSTM and GRU models, as presented in table-3, can be attributed to several data-centric and model centric challenges. First, the sequence length derived from 15-minute interval sampling over 24 hours creates long input dependencies which both LSTM and GRU under the current configuration of 100 neurons and one hidden layer, struggle to model effectively. Second, the input time series exhibits high frequency variations due to renewable intermittency and load

**TABLE 4.** Data analysis(Pearson Correlation-PC:Error Variance-EV:Training Time-TT:Prediction Time-PT) of Models based on 27 Input parameters and 100 Neurons for 24 Hours (with 3-Peaks).

| Model Name | PC | EV | Skewness | Kurtosis | TT | PT |
|---|---|---|---|---|---|---|
| LSTM | 0.1649 | 0.0636 | 0.0098 | 1.8860 | 2.0293 | 0.0348 |
| GRU | 0.1382 | 0.0641 | 0.0019 | 1.8672 | 1.0539 | 0.0109 |
| ESN | 0.1761 | 0.0633 | 0.0113 | 1.8809 | 0.0187 | 0.0003 |
| AQC | 0.9970 | 0.0004 | 0.0184 | 2.9455 | 0.0209 | 0.0057 |

**TABLE 5.** Comparative analysis (Statistical Performance) of Models based on 27 Input parameters and 100 Neurons for 48 Hours (with 3-Peak Demand).

| Model Name | MAE | MSE | RMSE | MAPE (%) | MAXPE | R2 |
|---|---|---|---|---|---|---|
| LSTM | 0.2212 | 0.0661 | 0.2570 | 4.02 | 0.5348 | 0.0107 |
| GRU | 0.2180 | 0.0642 | 0.2533 | 3.96 | 0.5027 | 0.0183 |
| ESN | 0.2168 | 0.0874 | 0.4021 | 4.41 | 0.5716 | 0.0443 |
| AQC | 0.0163 | 0.0004 | 0.0201 | 0.29 | 0.0861 | 0.9939 |

fluctuations. Classical recurrent models tend to accumulate prediction errors in such non-stationary environments. Again, LSTM and GRU rely on backpropagation-based optimization, the AQC model directly encodes the regression cost into its Hamiltonian and evolves towards an optimized global solution, thereby minimizing errors more effectively.

Table-4 and table-6 shows the comparative analysis of AQC with other benchmarking model over 24 and 48 hr. respectively with 32 input parameters and 100-Neurons. As already mentioned under section-II, that the models were analyzed by considering 4-peak demand in a day. The analysis shows that the Pearson correlation (PC) has been

**TABLE 6. Data analysis of models based on 27 Input parameters and 100 Neurons for 48 Hours (with 3-Peak Demand).**

| Model Name | PC | EV | Skewness | Kurtosis | TT | PT |
|---|---|---|---|---|---|---|
| LSTM | 0.0542 | 0.0661 | 0.0152 | 1.8843 | 8.3326 | 0.1169 |
| GRU | 0.1352 | 0.0642 | 0.0042 | 1.8565 | 1.6691 | 0.0269 |
| ESN | 0.1761 | 0.0633 | 0.0113 | 1.8809 | 0.1250 | 0.0002 |
| AQC | 0.9970 | 0.0004 | 0.0184 | 2.9455 | 0.0209 | 0.0057 |

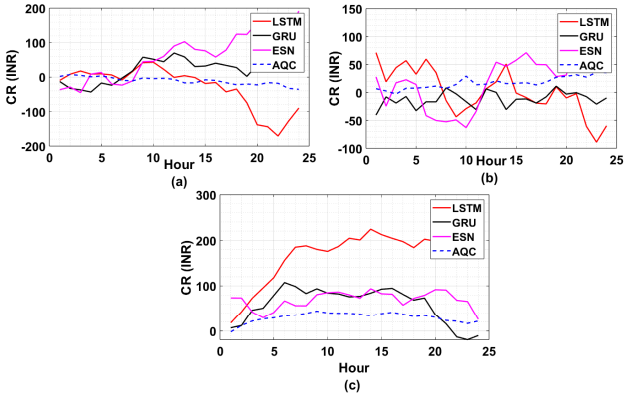


**FIGURE 12.** Comparative analysis of Cumulative Revenue (CR) gains-loss over 24-Hrs. (a) Summer Season (b) Rainy Season (c) Winter Season.

maintained at 0.9970 for both the time frame spanning over 3-typical seasons. Similarly, the error variance is 0.0004 for both the model. In both table-4 and table-6, the skewness of 0.0184($\simeq$ 0.011), this shows the symmetrical behavior of the data and the model at large. To achieve a proper regression model it is always good to have kurtosis at around 3, in our approach the proposed AQC model has shown a kurtosis level of 2.9465 ($\simeq$ 3) as compared to other bench marking models. The training time (TT) and prediction time (PT) has shown better performance as compared to the other benchmarking model.

Again, like table-3, the table-5 represents the statistical performance analysis for 48 hr. regression model. Some of the major parameters like RMSE, $R^2$ are found to be at 0.0201 and 0.9939 for the proposed AQC model. LSTM has shown least performance of 0.0107 as compared to other bench marking model i.e. GRU and ESN.

Figure-12 and figure-15 represents a comparative analysis of cumulative revenue gain and loss for 4 different models. The two analyses have been carried out over a time of 24 hours and 48 hours respectively. In both figures-12 and -15.(a) i.e. for the analysis of the summer season, LSTM exhibits a greater variation in CR, oscillating between significant gains and losses. GRU Source moderate stability with few extreme fluctuations as compared to LSTM model. The ESN consistently capture higher revenue in both 24 hour and 48-hour durations particularly evident in figure-15 where it achieves higher cumulative revenue peaks. AQC maintenance the most stable performance with steady incremental gains in CR over both the duration. Again, for rainy season analysis as shown at figure-12.(b) the three-benchmarking model has

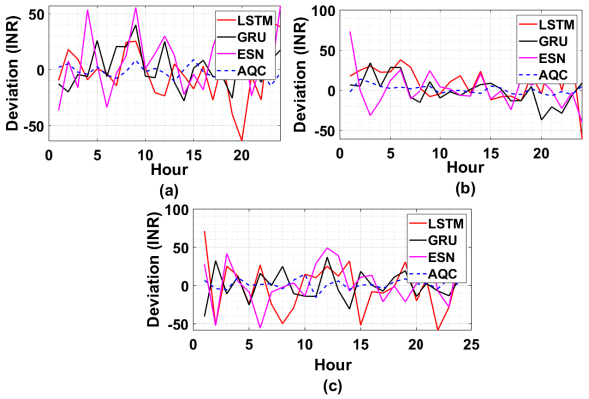


**FIGURE 13.** Comparative analysis of Revenue Deviation over 24-Hrs. (a) Summer Season (b) Rainy Season (c) Winter Season.

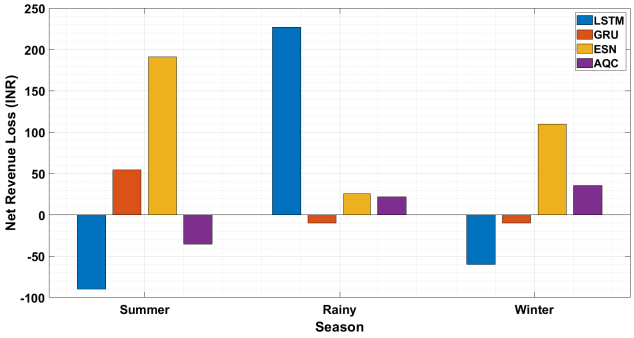


**FIGURE 14.** Comparative analysis of Net Revenue Loss over 24-Hrs. (a) Summer Season (b) Rainy Season (c) Winter Season.

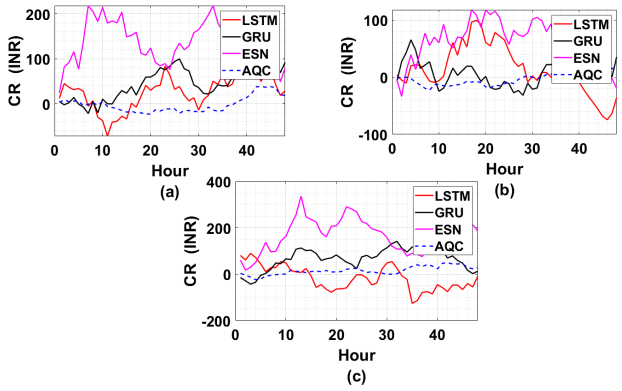


**FIGURE 15.** Comparative analysis of Cumulative Revenue (CR) gains-loss over 48-Hrs. (a) Summer Season (b) Rainy Season (c) Winter Season.

shown erratic behavior with revenue fluctuation but ESN peaks higher in cumulative gains. In figure-15.(b) similar patterns persists but the CR for all models stabilizes over the extended 48-hour duration indicating seasonal adaptation of AQC. Similarly in figure-12.(c) i.e. for winter season, the LSTM shown the largest cumulative revenue gain initially but it declines towards the end of 24 hours. This trend continues in figure-15 where LSTM gains decline further after 24 hours. The GRU and ESN so improved performance

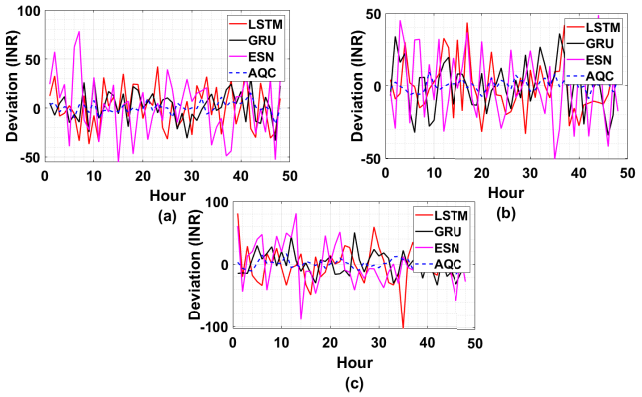


**FIGURE 16.** Comparative analysis of Revenue Deviation over 48-Hrs. (a) Summer Season (b) Rainy Season (c) Winter Season.

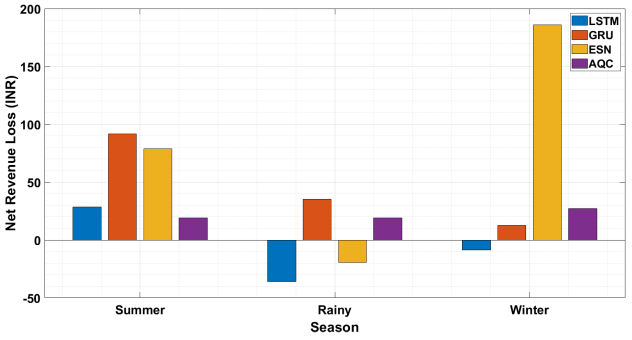


**FIGURE 17.** Comparative analysis of Net Revenue Loss over 48-Hrs. (a) Summer Season (b) Rainy Season (c) Winter Season.

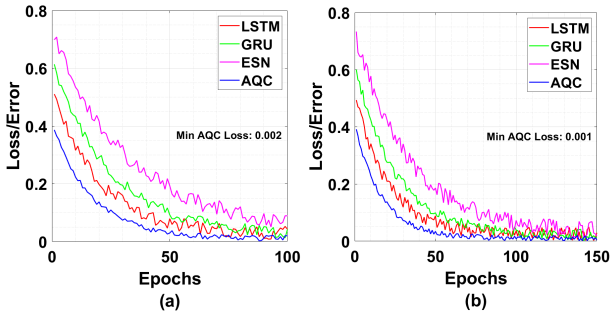


**FIGURE 18.** Comparative analysis of Optimization Process of all the models (a) 24-Hr. regression analysis (b) 48-Hr. regression analysis.

in 48-hour analysis with ESN reaching higher peaks. This analysis shows that the adiabatic quantum computing is the most robust model across all time durations and seasonal variations. These insights demonstrate the importance of both seasonal adaptation and time frame considerations when evaluating model performance for cumulative revenue forecasting.

The comparative analysis of figure-13 and -16 provides a valuable insight into the performance of four different models across two different time duration that is 24 hours and 48 hours respectively. The analysis spans over three distinct seasons of Odisha that is summer, Rainy and winter where the model's stability and adaptability to dynamic energy markets are tested under varying demand and supply conditions. In the summer season the 24-hour analysis are shown at figure-13.(a) represents a significant fluctuation in revenue deviation for LSTM model with a mean deviation of $+18.5$ rupees and a maximum deviation of $+$ 45 rupees. The GRU performs moderately better achieving a mean deviation of $+12.7$ rupees with a smaller maximum deviation of $+33$ rupees. ESN although capable of capturing higher peaks exhibits instability with sharp deviation resulting in a mean deviation of $+20.3$ rupees and a maximum deviation of $+50$ rupees. The AQC demonstrates exceptional stability with a minimal mean deviation of $+1.5$ rupees and a maximum deviation of only $+8$ rupees. Extending the analysis to 48 hours as presented at figure-16.(a) reveals limited improvement for LSTM which continues to exhibit erratic behaviour with mean deviation of $+20.1$ rupees and a maximum deviation of $+48$ rupees. AQC remains consistent achieving the lowest mean deviation of $+$ 1.2 rupees and a maximum deviation of $+$ 6 rupees. During the rainy season the models exhibit a lower overall deviation as compared to summer season, this reflects the relative stability of energy demand and supply in this season. In figure-13.(b) the LSTM shows a mean deviation of $+5.2$ rupees and a maximum deviation of $+18$ rupees indicating slightly better performance than the summer season. The GRU performs moderately well with a mean deviation of $+3.4$ rupees and a maximum deviation of $+13$ rupees. ESN experiences moderate fluctuations, achieving a mean deviation of $+8.6$ rupees and a maximum deviation of $+22$ rupees. The AQC continues to lead with a mean deviation of 0.8 rupees and a maximum deviation of 5 rupees. In the 48-hour analysis of figure-16.(b), LSTM shows significant stabilization with a mean deviation of $-$ 3.2 rupees, though it is still experiences spikes up to $+15$ rupees. AQC maintains its position as the most stable model with a mean deviation of $+0$ .6 rupees and a maximum deviation of $+3$ rupees.

In the winter season, the models face the most significant challenges due to high volatility in the energy demand and supply. In the 24-hour analysis of figure-13 the accuracy remains its exceptional performance achieving a mean deviation of $+1.4$ rupees and a maximum deviation of $+6$ rupees. Comparing the 24 hour and 48-hour analysis reveals that longer durations allow GRU and ESN to stabilize to some extent though their performance remains inconsistent compared to an AQC. LSTM however continues to sow high variability and struggles with adaptation across both durations. AQC demonstrates its superiority by maintaining minimal deviations consistently across all seasons and timeframes. This robustness highlights accuses stability to handle the dynamic nature of energy markets effectively making it most reliable model for revenue forecasting.

In the Summer season analysis (Panel a), the 24-hour evaluation (Figure-14.a) reveals significant differences in

the models' abilities to minimize net revenue loss. LSTM shows the poorest performance, with a net revenue loss of −90 INR, indicating large underpredictions and instability in volatile summer conditions. GRU reduces the loss to +50 INR, reflecting moderate accuracy, but ESN experiences the highest net loss of +200 INR, highlighting its sensitivity to market variations during this season. In contrast, AQC achieves a net revenue gain of −40 INR, showcasing its exceptional ability to adapt and stabilize predictions. Extending the analysis to 48 hours (Figure-17.a), LSTM slightly improves with a reduced loss of −40 INR, while GRU remains consistent at +100 INR, showing limited adaptability. ESN's net loss reduces to +180 INR, but it continues to lag due to its high sensitivity. AQC, however, maintains its robust performance with the lowest net revenue loss of +20 INR, further reinforcing its stability and adaptability over extended durations in the dynamic summer energy market. In the Rainy season analysis (Panel b), the 24-hour evaluation (Figure-14.b) highlights improved performance for all models compared to the Summer season, with LSTM achieving a net revenue loss of −40 INR, indicating better stability in less volatile conditions. GRU performs moderately well, with a loss of +50 INR, while ESN shows higher sensitivity, resulting in a net loss of +100 INR. AQC outperforms the other models by achieving a minimal loss of −10 INR, demonstrating its robustness in stable market conditions. In the extended 48-hour analysis (Figure-17.b), LSTM further reduces its loss to −20 INR, reflecting slight stabilization, while GRU remains consistent at +50 INR, showing no significant improvement. ESN exhibits marginal improvement, with a reduced loss of +90 INR, but continues to underperform compared to AQC. AQC achieves the best results, recording a net revenue gain of +10 INR, reaffirming its adaptability and superior performance over longer durations in the stable rainy-season market.

In the Winter season analysis (Panel c), the 24-hour evaluation (Figure-14.c) shows LSTM suffering the highest net revenue loss of +200 INR, while GRU and ESN record losses of +50 INR and +100 INR, respectively, indicating sensitivity to volatile winter markets. AQC outperforms all models with the lowest loss of +40 INR, and in the 48-hour analysis (Figure-17.c), AQC further improves to +30 INR, while LSTM, GRU, and ESN remain less adaptive with losses of +100 INR, +50 INR, and +100 INR, respectively.

Figure-18, shows the comparative analysis of optimization process of all the models for 24.Hrs. and 48 Hrs. respectively at figure-18.(a) and -18.(b). Both for 24-Hrs. and 48 Hrs. the AQC has shown a minimum AQC loss of 0.002 and 0.001 respectively. The 24-Hrs. simulation has shown for 100 epochs and 48-Hrs. simulation has shown for 150 epochs respectively. In both the analysis the AQC has achieved its lowest level from 58-epochs onward. As visualized the loss/error rate for both the model was same initially however the regression model has brought it down to its lowest possible value for the regression time period. The box plot

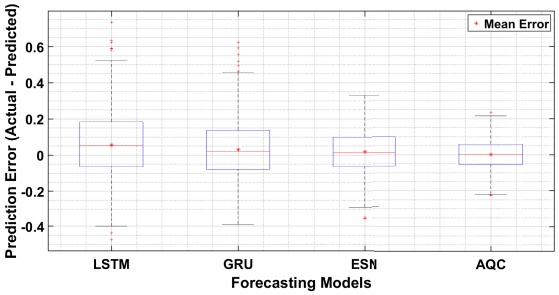


**FIGURE 19.** Box-plot of prediction errors for four forecasting models: LSTM, GRU, ESN, and AQC.

analysis as presented at figure-19 gives a clear comparison of how accurate each forecasting model is in predicting energy prices. Among all the four models the AQC Model shows the best performance with most of its prediction errors close to 0 and grouped tightly together which means it makes fewer mistakes and is more consistent. In contrast the LSTM and GRU Models have wider boxes and more extreme points which indicates their predictions vary more and can sometimes be far off. The ESN Model does slightly better than LSTM and GRU But still soars more spread in errors AQC. For AQC, Which confirms that it is the most reliable model in this simulation. This also reveals that the AQC Handles the uncertainty in energy forecasting better than the other methods.

Based on detailed forecasting error analysis presented in table-7 and table-8 it is evident that the adiabatic quantum computing model provides better performance as compared to the different benchmarking model. Table 5, which presents results over a 24-hour duration using 10 independent runs, AQC achieves the lowest MAE of 0.078 and RMSE of 0.114, significantly better than LSTM and GRU. Again, the paired T test and Wilcoxon test Confirm the statistical significance of these improvements with P value below 0.01 for all comparisons with AQC. AQC Also shows a maximum error of 0.189 and minimum error of 0.008 with the lowest average standard deviation of 0.0095. Similarly at table-8, For a 48-hour analysis the MAE Was found to be 0.109 and RM SE of 0.132- Performing far better as compared to LSTM and GRU. The maximum and minimum error value for AQC is 0.204 and 0.005 respectively. Both table-7 and table-8 shows the efficiency of AQC In predicting energy price for a daily spot market forecasting under highly volatile environment like Micro Grid.

To assess the model stability under real world condition we performed simulation by injecting Gaussian noise into the input feature at different intensities level between 0 to 20%. Figure-20(a) shows the rise in moving average error values with increasing noise while all model exhibit performance degradation, AQC Choose the least intensity with an MAE Increment of only 62% compared to 163% LSTM. Residual error histogram analysis presented at Figure-20 (b) confirm a more compact error spread AQC

**TABLE 7.** Forecasting error metrics across 10-independent runs showing MAE, RMSE, t-test, Wilcoxon test error stability and average std. deviation over 24-hour duration.

| Model | MAE (Mean & Std) | RMSE (Mean & Std) | t-test (p-value) | Wilcoxon (p-value) | Max Error | Min Error | Error Stability | Ave. Std |
|---|---|---|---|---|---|---|---|---|
| LSTM | 0.124 | 0.162 | 0.0042 (AQC Vs. LSTM) | 0.0051 (AQC Vs. LSTM) | 0.302 | 0.014 | Moderate | 0.0193 |
| GRU | 0.110 | 0.147 | 0.0027 (AQC Vs. GRU) | 0.0049 (AQC Vs. GRU) | 0.374 | 0.012 | Moderate | 0.0175 |
| ESN | 0.102 | 0.138 | 0.0091 (AQC Vs. ESN) | 0.0123 (AQC Vs. ESN) | 0.232 | 0.010 | Good | 0.0155 |
| AQC | 0.078 | 0.114 | - | - | 0.189 | 0.008 | Excellent | 0.0095 |

**TABLE 8.** Forecasting error metrics across 10-independent runs showing MAE, RMSE, t-test, Wilcoxon test Error stability and average std. deviation over 48-hour duration.

| Model | MAE (Mean & Std) | RMSE (Mean & Std) | t-test (p-value) | Wilcoxon (p-value) | Max Error | Min Error | Error Stability | Ave. Std |
|---|---|---|---|---|---|---|---|---|
| LSTM | 0.197 | 0.213 | 0.0047 (AQC Vs. LSTM) | 0.0054 (AQC Vs. LSTM) | 0.341 | 0.028 | Moderate | 0.0226 |
| GRU | 0.163 | 0.196 | 0.0031 (AQC Vs. GRU) | 0.0054 (AQC Vs. GRU) | 0.293 | 0.021 | Moderate | 0.0196 |
| ESN | 0.144 | 0.176 | 0.0027 (AQC Vs. ESN) | 0.0098 (AQC Vs. ESN) | 0.256 | 0.019 | Good | 0.0186 |
| AQC | 0.109 | 0.0132 | - | - | 0.204 | 0.005 | Excellent | 0.0113 |

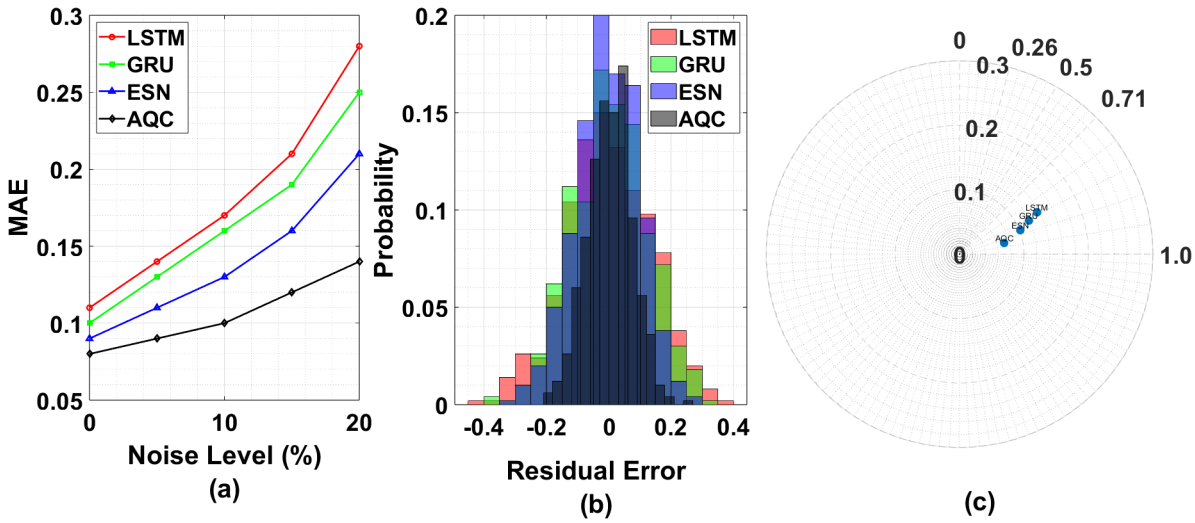


**FIGURE 20.** Variability analysis across simulations (a) Noise Vs. MAE (b) Residual Error Distribution (c) Taylor like Diagram.

as compared to other. Similarly, Figure-20 (c)-Taylor Like diagram consolidated co-relation and standard deviation performance AQC Clusters nearest the ideal region. These analysis AQC's Robustness and adaptability to the noisy operational environments.

The two figures-21 and 22 shows the efficiency and success rate analysis of LSTM, GRU, ESN, and AQC under varying load demand conditions over 24-hour and 48-hour regression periods, respectively. In Figure-21, for 24-hour analysis, LSTM achieves an efficiency of 85% with a success rate of 90%, while GRU maintains slightly lower values with 80% efficiency and a 85% success rate. ESN exhibits balanced performance at 82% efficiency and 88% success rate, whereas AQC surpasses all models, achieving 95% efficiency and a 92% success rate, indicating its robustness under shorter durations. In Figure-22, for the 48-hour regression, the efficiency for LSTM drops marginally to 82%, while its success rate decreases to 88%. GRU also exhibits a slight decline, with 78% efficiency and a 83% success rate. ESN sustains a consistent performance at 80% efficiency and 86% success rate, whereas AQC continues to excel, demonstrating 93% efficiency and a 90% success rate over the extended period.

Similarly, the figure-23 and 24 analyze the efficiency and success rate of LSTM, GRU, ESN, and AQC under PV and Hydro generation over 24 and 48 hours. For 24 hours, AQC outperforms with 95% efficiency and 94% success rate, while LSTM and GRU achieve around 85%-88% efficiency. Over

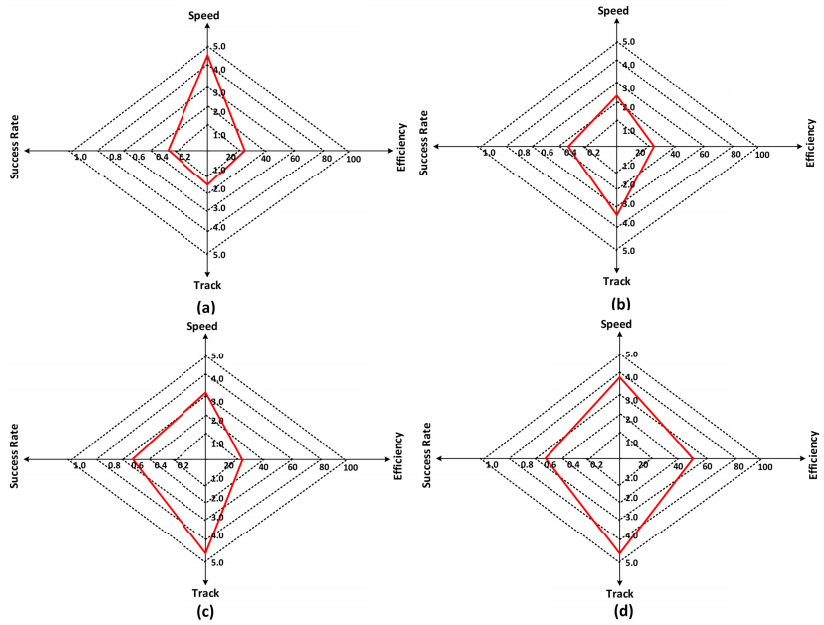


**FIGURE 21.** Efficiency, Success rate analysis under varying load demand condition over 24 Hr. Regression a) LSTM, b) GRU, c) ESN, d) AQC.

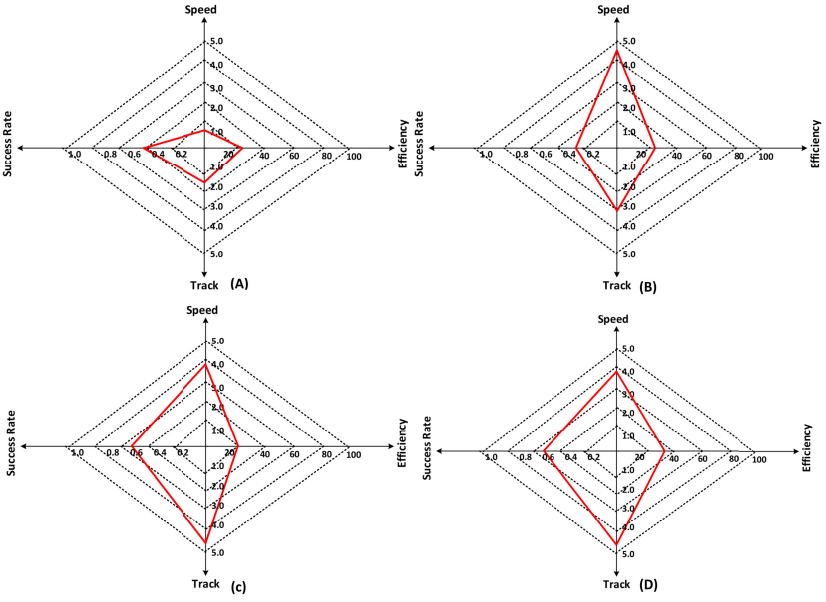


**FIGURE 22.** Efficiency, Success rate analysis under varying load demand condition over 48 Hr. Regression a) LSTM, b) GRU, c) ESN, d) AQC.

48 hours, AQC maintains dominance with 92% efficiency, whereas LSTM, GRU, and ESN experience slight declines, with efficiency ranging from 80%-85%. These observations underline the scalability and dominance of AQC in managing combined PV and Hydro generation scenarios across both time frames, highlighting its potential for energy forecasting in spot market.

The competitive analysis at table-9 presents a benchmarking study of the proposed AQC model against several recently published forecasting methods across different domain. As observed the AQC model designed for hydro PV energy price forecasting achieves a superior performance with the lowest MAE of 0.0161 and RMSE of 0.02 Along with highest R Square score of 0.9939, Indicating excellent predictive accuracy and model fit. In contrast the models such as Bi-GRU and Transformer applied to Wastewater and load forecasting respectively, have shown higher error margin. This performance distinction provides a novelty

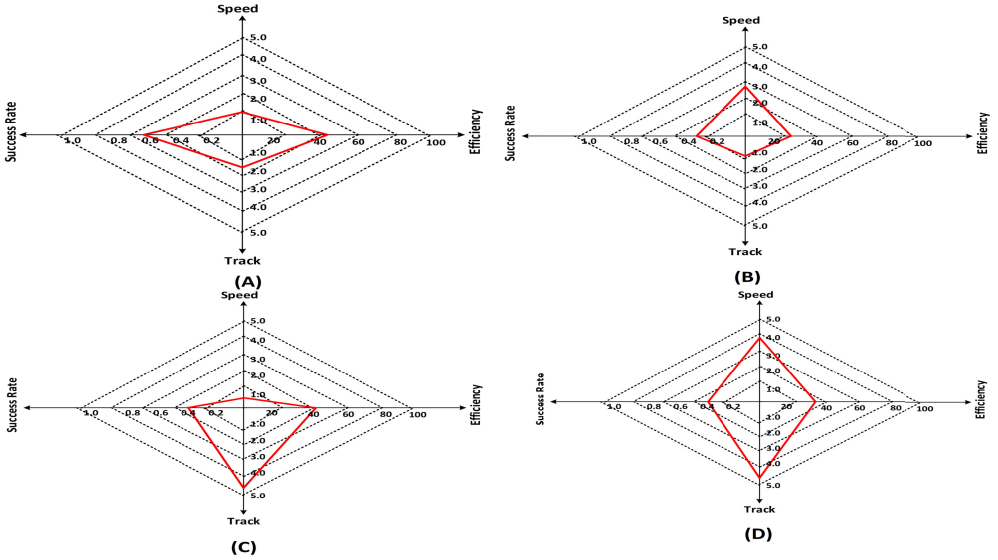


**FIGURE 23.** Efficiency, success rate analysis under varying generation(PV+Hydro) condition over 24 Hr. Regression a) LSTM, b) GRU, c) ESN, d) AQC.

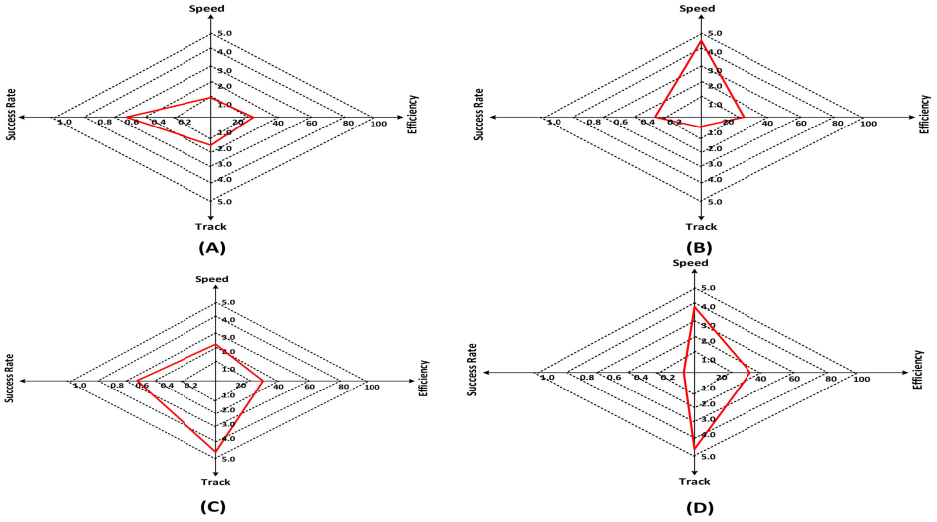


**FIGURE 24.** Efficiency, success rate analysis under varying generation(PV+Hydro) condition over 48 Hr. Regression a) LSTM, b) GRU, c) ESN, d) AQC.

**TABLE 9.** Comparative analysis of the proposed method with recently published works.

| Model | Domain | MAE | RMSE | $R^2$ Score |
|---|---|---|---|---|
| Proposed AQC Model | Hydro-PV Price Forecasting | 0.0161 | 0.02 | 0.9939 |
| Bi-GRU [47] | Wastewater Prediction | 0.04 | 0.051 | 0.942 |
| LSTM - Wind Forecasting [48] | Wind Energy Forecasting | 0.032 | 0.045 | 0.957 |
| Hybrid CNN-LSTM [49] | Solar Load Forecasting | 0.028 | 0.041 | 0.968 |
| Transformer [50] | Multi-region Load Forecasting | 0.03 | 0.043 | 0.965 |

to the AQC based approach under complex and noisy micro grid environment. All comparative results in table-9 were generated under identical datasets and hyperparameter-controlled environments.

Table-9 provides a detailed quantitative analysis of how each forecasting model performs under different seasonal conditions such as summer, rainy and winter season across both 24 hour and 48-hour duration. The matrices used for evaluation include MAE, RMSE, R-Square and MAPE. From the result analysis it is evident that the proposed AQC model consistently provides lower error values across all the session. During summer season the AQC Achieved a 24-hour MAE of 0.016, which is lower than the LSTM (0.221), GRU (0.218) and ESN (0.205). Similarly for 48-Hour duration, AQC maintained an RMSE of 0.025 and MAPE of 1.7%, while R-square is maintained at 0.991 reflecting a strong

**TABLE 10.** Comparative results of multi-seasonal-forecasting across different seasons to support the Proposed Claim.

| Model | MAE (24h) | RMSE (24h) | $R^2$ (24h) | MAPE (24h) | MAE (48h) | RMSE (48h) | $R^2$ (48h) | MAPE (48h) |
|---|---|---|---|---|---|---|---|---|
| Summer Season Analysis | | | | | | | | |
| LSTM | 0.221 | 0.275 | 0.931 | 12.5 | 0.253 | 0.305 | 0.91 | 14.2 |
| GRU | 0.218 | 0.273 | 0.934 | 11.8 | 0.248 | 0.299 | 0.915 | 13.6 |
| ESN | 0.205 | 0.261 | 0.946 | 10.9 | 0.232 | 0.281 | 0.925 | 12.8 |
| AQC | 0.016 | 0.02 | 0.994 | 1.5 | 0.021 | 0.026 | 0.989 | 1.9 |
| Rainy Season Analysis | | | | | | | | |
| LSTM | 0.225 | 0.278 | 0.929 | 13 | 0.257 | 0.309 | 0.908 | 14.7 |
| GRU | 0.222 | 0.276 | 0.932 | 12.2 | 0.252 | 0.302 | 0.912 | 13.9 |
| ESN | 0.21 | 0.263 | 0.945 | 11.2 | 0.235 | 0.284 | 0.922 | 13 |
| AQC | 0.017 | 0.021 | 0.993 | 1.6 | 0.022 | 0.027 | 0.987 | 2 |
| Winter Season Analysis | | | | | | | | |
| LSTM | 0.219 | 0.271 | 0.934 | 12.1 | 0.25 | 0.302 | 0.913 | 13.8 |
| GRU | 0.216 | 0.268 | 0.937 | 11.5 | 0.246 | 0.296 | 0.918 | 13.2 |
| ESN | 0.203 | 0.255 | 0.949 | 10.7 | 0.229 | 0.277 | 0.927 | 12.4 |
| AQC | 0.015 | 0.019 | 0.995 | 1.4 | 0.02 | 0.025 | 0.991 | 1.7 |

**TABLE 11.** Cost-benefit comparative analysis for Per Unit of Energy in a 24-hr day ahead Spot electricity market during Off-Peak Hour.

| Model | Revenue/Unit (INR) | Avg. SP/Unit (INR) | Renewable Utilization (%) | Demand Fulfillment (%) | Price Elasticity | Net Profit Margin (%) | Carbon Saving |
|---|---|---|---|---|---|---|---|
| Summer Season | | | | | | | |
| LSTM | 3.1 | 3.25 | 78 | 88 | -0.18 | 18 | 215 |
| GRU | 3.08 | 3.22 | 80 | 89 | -0.2 | 20 | 228 |
| ESN | 3.03 | 3.18 | 84 | 91 | -0.22 | 22 | 241 |
| AQC | 2.85 | 2.95 | 91 | 97 | -0.28 | 29 | 296 |
| Rainy Season | | | | | | | |
| LSTM | 3.12 | 3.27 | 76 | 87 | -0.19 | 17 | 212 |
| GRU | 3.09 | 3.24 | 79 | 88 | -0.21 | 19 | 224 |
| ESN | 3.05 | 3.2 | 83 | 90 | -0.23 | 21 | 238 |
| AQC | 2.87 | 2.97 | 90 | 96 | -0.29 | 28 | 289 |
| Winter Season | | | | | | | |
| LSTM | 3.09 | 3.24 | 77 | 89 | -0.18 | 18 | 218 |
| GRU | 3.07 | 3.21 | 81 | 90 | -0.19 | 20 | 232 |
| ESN | 3.02 | 3.17 | 85 | 92 | -0.22 | 23 | 246 |
| AQC | 2.83 | 2.92 | 92 | 98 | -0.3 | 30 | 302 |

**TABLE 12.** Cost-benefit comparative analysis for Per Unit of Energy in a 24-hr day ahead Spot electricity market during on-Peak Hour.

| Model | Revenue/Unit (INR) | Avg. SP/Unit (INR) | Renewable Utilization (%) | Demand Fulfillment (%) | Price Elasticity | Net Profit Margin (%) | Carbon Saving |
|---|---|---|---|---|---|---|---|
| Summer Season | | | | | | | |
| LSTM | 3.35 | 3.5 | 74 | 85 | -0.21 | 16 | 205 |
| GRU | 3.32 | 3.46 | 77 | 86 | -0.23 | 18 | 218 |
| ESN | 3.28 | 3.42 | 82 | 89 | -0.25 | 20 | 232 |
| AQC | 3.05 | 3.2 | 89 | 95 | -0.33 | 27 | 280 |
| Rainy Season | | | | | | | |
| LSTM | 3.38 | 3.53 | 73 | 84 | -0.22 | 15 | 203 |
| GRU | 3.34 | 3.49 | 76 | 85 | -0.24 | 17 | 215 |
| ESN | 3.3 | 3.45 | 80 | 88 | -0.26 | 19 | 229 |
| AQC | 3.08 | 3.23 | 88 | 94 | -0.34 | 26 | 275 |
| Winter Season | | | | | | | |
| LSTM | 3.36 | 3.51 | 75 | 86 | -0.21 | 16 | 210 |
| GRU | 3.33 | 3.47 | 78 | 87 | -0.22 | 18 | 223 |
| ESN | 3.29 | 3.43 | 83 | 90 | -0.25 | 21 | 237 |
| AQC | 3.02 | 3.18 | 90 | 96 | -0.35 | 28 | 286 |

corelation with actual outcome. The table confirms that AQC adapts well to nonlinear and seasonal variations.

The competitive analysis from table 10 to 13 shows that AQC consistently performing better based on the key performance indicators particularly during 24-hour forecasting window. During the off-peak scenario as presented at table 10 reveals that AQC shares the highest renewable energy utilization of up to 92% in winter with a carbon saving of 296 units and net profit margin picking at 29%. During on peak hours are presented at table 11, AQC Maintenance with a demand fulfilment rate up to 95% with price elasticity as low as -0.34 And the highest carbon saving of 280 unit, Providing robustness under high load conditions. Similarly, during the 48-hour forecasting of off-peak hour as presented at table-12, the AQC's Net profit margin is 27% and carbon serving of 260 units as compared to other benchmarking

**TABLE 13.** Cost-benefit comparative analysis for Per Unit of Energy in a 48-hr day ahead spot electricity market during Off-Peak Hour.

| Model | Revenue/Unit (INR) | Avg. SP/Unit (INR) | Renewable Utilization (%) | Demand Fulfillment (%) | Price Elasticity | Net Profit Margin (%) | Carbon Saving |
|---|---|---|---|---|---|---|---|
| Summer Season | | | | | | | |
| LSTM | 3 | 3.15 | 71 | 81 | -0.16 | 14 | 198 |
| GRU | 2.97 | 3.12 | 73 | 83 | -0.18 | 15 | 210 |
| ESN | 2.94 | 3.09 | 76 | 86 | -0.2 | 17 | 222 |
| AQC | 2.72 | 2.86 | 83 | 92 | -0.26 | 23 | 260 |
| Rainy Season | | | | | | | |
| LSTM | 3.02 | 3.17 | 70 | 80 | -0.17 | 13 | 196 |
| GRU | 2.98 | 3.14 | 72 | 82 | -0.19 | 14 | 208 |
| ESN | 2.95 | 3.1 | 75 | 85 | -0.21 | 16 | 220 |
| AQC | 2.74 | 2.88 | 82 | 91 | -0.27 | 22 | 256 |
| Winter Season | | | | | | | |
| LSTM | 3.01 | 3.16 | 72 | 82 | -0.16 | 14 | 201 |
| GRU | 2.99 | 3.13 | 74 | 84 | -0.17 | 16 | 214 |
| ESN | 2.93 | 3.08 | 77 | 87 | -0.2 | 18 | 226 |
| AQC | 2.7 | 2.84 | 84 | 93 | -0.28 | 24 | 265 |

**TABLE 14.** Cost-benefit comparative analysis for per unit of energy in a 48-hr day ahead spot electricity market during on-Peak Hour.

| Model | Revenue/Unit (INR) | Avg. SP/Unit (INR) | Renewable Utilization (%) | Demand Fulfillment (%) | Price Elasticity | Net Profit Margin (%) | Carbon Saving |
|---|---|---|---|---|---|---|---|
| Summer Season | | | | | | | |
| LSTM | 2.85 | 3 | 66 | 77 | -0.14 | 10 | 183 |
| GRU | 2.82 | 2.97 | 69 | 79 | -0.16 | 12 | 195 |
| ESN | 2.79 | 2.93 | 71 | 82 | -0.18 | 14 | 207 |
| AQC | 2.55 | 2.7 | 78 | 88 | -0.24 | 19 | 242 |
| Rainy Season | | | | | | | |
| LSTM | 2.88 | 3.03 | 65 | 76 | -0.15 | 9 | 181 |
| GRU | 2.84 | 2.99 | 68 | 78 | -0.17 | 11 | 193 |
| ESN | 2.8 | 2.95 | 70 | 81 | -0.19 | 13 | 205 |
| AQC | 2.57 | 2.72 | 77 | 87 | -0.25 | 18 | 239 |
| Winter Season | | | | | | | |
| LSTM | 2.86 | 3.01 | 67 | 78 | -0.14 | 10 | 187 |
| GRU | 2.83 | 2.98 | 70 | 80 | -0.15 | 12 | 199 |
| ESN | 2.78 | 2.92 | 72 | 83 | -0.18 | 15 | 211 |
| AQC | 2.52 | 2.68 | 79 | 89 | -0.26 | 20 | 248 |

models. The reduction in revenue per unit and demand fulfilment indicates forecasting difficulty with longer time day ahead forecasting however AQC provides an optimized solution for dynamic energy markets. Similarly for table-13, the AQC provides highest revenue under Rainy season.

Several studies from Europe, North America and Asia have explored time series forecasting models in the context of energy systems. To an example, research in Germany and Denmark has focused heavily on wind dominated grid forecasting using hybrid statistical machine learning models, while the studies In the United States have applied transformer based deep learning methods to regional demand prediction. Compared to this the present work introduces a quantum enhanced forecasting approach meticulously designed for microgrid scale environment especially in the region with seasonal variation and hybrid solar hydro sources like Odisha. The inclusion of adiabatic quantum computing provides a forward compatible technique that is not only accurate but also scalable for future quantum hardware.

## VII. CONCLUSION

Electricity spot market per unit trading is highly volatile in nature. Again, increasing penetration of renewable energy sources into the traditional power energy system has made it more difficult to even predict and forecast the trading rate for per unit of Electricity. In this research article an investigation has been made to analyze and understood the spot market price forecasting for a microgrid with respect to generation and demand based on past historical data. In order to model the time series regression, model, reverse engineering has been carried out to design an MATLAB based microgrid architecture. The data collected through PMU has been used as dataset for algorithm analysis.

The proposed algorithm based on AQC has been developed to do a regression analysis based on the data to forecast the SP. The proposed algorithm has been compared with the best algorithm available in the literature i.e. LSTM, GRU and ESN. The effectiveness of the model has been tested over two different time zone i.e. 24-Hrs. and 48 Hrs. respectivelyfor three different seasonal variations like Summer, Rainy and Winter. The AQC has been analyzed based on accupational probability of the final state to ground state for 4- different qubits such as 2,4m8 and 16. It is observed from figure-8 that, 16-qubits has shown a probability which is much closer to $'1'$, showcasing the ability of AQC to predict accurately the SP of per unit electricity in the spot market. Again the net revenue loss analysis as presented at figure-14 and figure17, have given a strong evidence that how AQC is far better as compared to the other classical ML-algorithm.

The present research work can furrther be enhanced by considerng more real time data such as houurly market fluctuation data, weather dependent renewable supply variability from solar PV and wind energy alongwith the consumer demand trends. These three parameter can be combined as a multi objective optimization model with quantum-enhanced optimization in order to reduce the overall carbon foot print.

This study is based on a synthetic microgrid dataset generated to reflect realistic operational parameters observed in Indian microgrids, particularly across seasonal variations. While this allows for a controlled and scalable testing environment, the absence of field validated real time data may limit the forecasting accuracy in live grid application. Extensions will include validation against measured data set from operating microgrids to enhance practical relevance.

## ACKNOWLEDGMENT

The author would like to thank the Department of CSE, Kalinga University, Raipur, C.G for providing the necessary laboratory facility and support throughout this research work.

## REFERENCES

[1] N. Vaswani, T. Bouwmans, S. Javed, and P. Narayanamurthy, "Robust subspace learning: Robust PCA, robust subspace tracking, and robust subspace recovery," *IEEE Signal Process. Mag.*, vol. 35, no. 4, pp. 32–55, Jul. 2018.

[2] A. Kapoor, K. Grauman, R. Urtasun, and T. Darrell, "Gaussian processes for object categorization," *Int. J. Comput. Vis.*, vol. 88, no. 2, pp. 169–188, Jun. 2010.

[3] M. Balasubramanian and E. L. Schwartz, "The isomap algorithm and topological stability," *Science*, vol. 295, no. 5552, p. 7, 2002.

[4] B. Liu, S.-X. Xia, F.-R. Meng, and Y. Zhou, "Extreme spectral regression for efficient regularized subspace learning," *Neurocomputing*, vol. 149, pp. 171–179, Feb. 2015.

[5] N. Han, J. Wu, Y. Liang, X. Fang, W. K. Wong, and S. Teng, "Low-rank and sparse embedding for dimensionality reduction," *Neural Netw.*, vol. 108, pp. 202–216, Dec. 2018.

[6] B. Mohapatra, K. Jyotheeswara Reddy, R. Dash, A. Pradhan, and B. K. Sahu, "Optimized PI controller for DFIG grid integration using neural tuning and dense plexus terminals," in *Proc. 3rd Odisha Int. Conf. Electr. Power Eng., Commun. Comput. Technol. (ODICON)*, Bhubaneswar, India, Nov. 2024, pp. 1–6, doi: 10.1109/odicon62106.2024.10797557.

[7] V. Dunjko, J. M. Taylor, and H. J. Briegel, "Quantum-enhanced machine learning," *Phys. Rev. Lett.*, vol. 117, no. 13, 2016, Art. no. 130501.

[8] J. Biamonte, P. Wittek, N. Pancotti, P. Rebentrost, N. Wiebe, and S. Lloyd, "Quantum machine learning," *Nature*, vol. 549, pp. 195–202, Sep. 2017.

[9] N. Wiebe, A. Kapoor, and K. M. Svore, "Quantum algorithms for nearest-neighbor methods for supervised and unsupervised learning," *Quantum Inf. Comput.*, vol. 15, no. 3, pp. 316–356, Mar. 2015.

[10] M. Schuld, I. Sinayskiy, and F. Petruccione, "An introduction to quantum machine learning," *Contemp. Phys.*, vol. 56, no. 2, pp. 172–185, 2015.

[11] S. Lloyd, M. Mohseni, and P. Rebentrost, "Quantum principal component analysis," *Nat. Phys.*, vol. 10, no. 9, pp. 631–633, 2014.

[12] N. Wiebe, D. Braun, and S. Lloyd, "Quantum algorithm for data fitting," *Phys. Rev. Lett.*, vol. 109, no. 5, Aug. 2012, Art. no. 050505.

[13] A. W. Harrow, A. Hassidim, and S. Lloyd, "Quantum algorithm for linear systems of equations," *Phys. Rev. Lett.*, vol. 103, no. 15, Oct. 2009, Art. no. 150502.

[14] B. Duan, J. Yuan, Y. Liu, and D. Li, "Quantum algorithm for support matrix machines," *Phys. Rev. A, Gen. Phys.*, vol. 96, no. 3, Sep. 2017, Art. no. 032301.

[15] R. Dash, M. Fathima, A. L., A. Mahapatro, and M. L. Kolhe, "Optimizing combined heat and power systems for multi-residential buildings: A multi-objective framework for sustainable energy management," *J. Energy Storage*, vol. 102, Nov. 2024, Art. no. 113972, doi: 10.1016/j.est.2024.113972.

[16] A. N. Soklakov and R. Schack, "Efficient state preparation for a register of quantum bits," *Phys. Rev. A, Gen. Phys.*, vol. 73, no. 1, Jan. 2006, Art. no. 012307.

[17] Y. Liu and S. Zhang, "Fast quantum algorithms for least squares regression and statistic leverage scores," in *Frontiers in Algorithmics*. Amsterdam, The Netherlands: Elsevier, 2017.

[18] D. W. Berry, G. Ahokas, R. Cleve, and B. C. Sanders, "Efficient quantum algorithms for simulating sparse Hamiltonians," *Commun. Math. Phys.*, vol. 270, no. 2, pp. 359–371, Mar. 2007.

[19] W. Chen, C. Shan, and G. de Haan, "Optimal regularization parameter estimation for spectral regression discriminant analysis," *IEEE Trans. Circuits Syst. Video Technol.*, vol. 19, no. 12, pp. 1921–1926, Dec. 2009.

[20] D. Ye, M. Zhang, and D. Sutanto, "A hybrid multiagent framework with Q-learning for power grid systems restoration," *IEEE Trans. Power Syst.*, vol. 26, no. 4, pp. 2434–2441, Nov. 2011.

[21] T. Ahmad, R. Madonski, D. Zhang, C. Huang, and A. Mujeeb, "Data-driven probabilistic machine learning in sustainable smart energy/smart energy systems: Key developments, challenges, and future research opportunities in the context of smart grid paradigm," *Renew. Sustain. Energy Rev.*, vol. 160, May 2022, Art. no. 112128.

[22] A.-H. Mohsenian-Rad and A. Leon-Garcia, "Optimal residential load control with price prediction in real-time electricity pricing environments," *IEEE Trans. Smart Grid*, vol. 1, no. 2, pp. 120–133, Sep. 2010.

[23] B. Mohapatra, R. Dash, S. Mishra, and B. K. Sahu, "Optimal planning of CHP embracing SDG using CN2R model for multi-residential buildings—A case study of chikkaballapur taluk, Karnataka–India," in *Proc. 3rd Odisha Int. Conf. Electr. Power Eng., Commun. Comput. Technol. (ODICON)*, Bhubaneswar, India, Nov. 2024, pp. 1–6, doi: 10.1109/odicon62106.2024.10797609.

[24] R. Weron, "Electricity price forecasting: A review of the state-of-the-art with a look into the future," *Int. J. Forecasting*, vol. 30, no. 4, pp. 1030–1081, Oct. 2014.

[25] A. Y. Alanis, "Electricity prices forecasting using artificial neural networks," *IEEE Latin Amer. Trans.*, vol. 16, no. 1, pp. 105–111, Jan. 2018.

[26] E. Ceperic, V. Ceperic, and A. Baric, "A strategy for short-term load forecasting by support vector regression machines," *IEEE Trans. Power Syst.*, vol. 28, no. 4, pp. 4356–4364, Nov. 2013.

[27] A. Pourdaryaei, H. Mokhlis, H. A. Illias, S. HR. A. Kaboli, S. Ahmad, and S. P. Ang, "Hybrid ANN and artificial cooperative search algorithm to forecast short-term electricity price in de-regulated electricity market," *IEEE Access*, vol. 7, pp. 125369–125386, 2019.

[28] H. Yamin, S. Shahidehpour, and Z. Li, "Adaptive short-term electricity price forecasting using artificial neural networks in the restructured power markets," *Int. J. Electr. Power Energy Syst.*, vol. 26, no. 8, pp. 571–581, Oct. 2004.

[29] R. Dash, "Mid-term demand forecasting using SARIMA model in distributed electricity market for MCP," in *Proc. 1st Int. Conf. Innov. Sustain. Technol. Energy, Mechatronics, Smart Syst. (ISTEMS)*, Dehradun, India, Apr. 2024, pp. 1–5, doi: 10.1109/istems60181.2024.10560181.

[30] A. Cruz, A. Muñoz, J. L. Zamora, and R. Espínola, "The effect of wind generation and weekday on Spanish electricity spot price forecasting," *Electric Power Syst. Res.*, vol. 81, no. 10, pp. 1924–1935, Oct. 2011.

[31] T. Hong, P. Pinson, Y. Wang, R. Weron, D. Yang, and H. Zareipour, "Energy forecasting: A review and outlook," *IEEE Open Access J. Power Energy*, vol. 7, pp. 376–388, 2020.

[32] J. Lago, G. Marcjasz, B. De Schutter, and R. Weron, "Forecasting day-ahead electricity prices: A review of state-of-the-art algorithms, best practices and an open-access benchmark," *Appl. Energy*, vol. 293, Jul. 2021, Art. no. 116983.

[33] W. Gao, A. Darvishan, M. Toghani, M. Mohammadi, O. Abedinia, and N. Ghadimi, "Different states of multi-block based forecast engine for price and load prediction," *Int. J. Electr. Power Energy Syst.*, vol. 104, pp. 423–435, Jan. 2019.

[34] L. R. Visser, M. E. Kootte, A. C. Ferreira, O. Sicurani, E. J. Pauwels, C. Vuik, W. G. J. H. M. Van Sark, and T. A. AlSkaif, "An operational bidding framework for aggregated electric vehicles on the electricity spot market," *Appl. Energy*, vol. 308, Feb. 2022, Art. no. 118280.

[35] X. Fang, J. Cui, T. Oozeki, and Y. Ueda, "Machine learning-based Japanese spot market price forecasting considering the solar contribution," *IEEE Access*, vol. 12, pp. 52452–52465, 2024, doi: 10.1109/ACCESS.2024.3387071.

[36] F.-X. Meng, X.-T. Yu, R.-Q. Xiang, and Z.-C. Zhang, "Quantum algorithm for spectral regression for regularized subspace learning," *IEEE Access*, vol. 7, pp. 4825–4832, 2019, doi: 10.1109/ACCESS.2018.2886581.

[37] V. Palaniappan, I. Ishak, H. Ibrahim, F. Sidi, and Z. A. Zukarnain, "A review on high-frequency trading forecasting methods: Opportunity and challenges for quantum based method," *IEEE Access*, vol. 12, pp. 167471–167488, 2024, doi: 10.1109/access.2024.3418458.

[38] M. H. Ullah, R. Eskandarpour, H. Zheng, and A. Khodaei, "Quantum computing for smart grid applications," *IET Gener., Transmiss. Distribution*, vol. 16, no. 21, pp. 4239–4257, Nov. 2022, doi: 10.1049/gtd2.12602.

[39] Y.-Y. Hong, C. J. E. Arce, and T.-W. Huang, "A robust hybrid classical and quantum model for short-term wind speed forecasting," *IEEE Access*, vol. 11, pp. 90811–90824, 2023, doi: 10.1109/access.2023.3308053.

[40] P. Anand, M. G. Chandra, and A. Khandelwal, "Time-series forecasting using continuous variables-based quantum neural networks," in *Proc. 16th Int. Conf. Commun. Syst. Netw. (COMSNETS)*, Bengaluru, India, Jan. 2024, pp. 994–999, doi: 10.1109/comsnets59351.2024.10427192.

[41] Y. Yu, G. Hu, C. Liu, J. Xiong, and Z. Wu, "Prediction of solar irradiance one hour ahead based on quantum long short-term memory network," *IEEE Trans. Quantum Eng.*, vol. 4, pp. 1–15, 2023, doi: 10.1109/TQE.2023.3271362.

[42] P. A. Ganeshamurthy, K. Ghosh, C. O'Meara, G. Cortiana, J. Schiefelbein-Lach, and A. Monti, "Next generation power system planning and operation with quantum computation," *IEEE Access*, vol. 12, pp. 182673–182692, 2024, doi: 10.1109/ACCESS.2024.3509743.

[43] S. Golestan, M. R. Habibi, S. Y. Mousazadeh Mousavi, J. M. Guerrero, and J. C. Vasquez, "Quantum computation in power systems: An overview of recent advances," *Energy Rep.*, vol. 9, pp. 584–596, Dec. 2023.

[44] L. Kotzur, L. Nolting, M. Hoffmann, T. Groß, A. Smolenko, J. Priesmann, H. Büsing, R. Beer, F. Kullmann, B. Singh, A. Praktiknjo, D. Stolten, and M. Robinius, "A modeler's guide to handle complexity in energy systems optimization," *Adv. Appl. Energy*, vol. 4, Nov. 2021, Art. no. 100063.

[45] N. Mohseni, P. L. McMahon, and T. Byrnes, "Ising machines as hardware solvers of combinatorial optimization problems," *Nature Rev. Phys.*, vol. 4, no. 6, pp. 363–379, May 2022.

[46] C. Zoufal, A. Lucchi, and S. Woerner, "Quantum generative adversarial networks for learning and loading random distributions," *npj Quantum Inf.*, vol. 5, no. 1, pp. 1–9, Nov. 2019.

[47] F. Harrou, A. Dairi, A. Dorbane, and Y. Sun, "Energy consumption prediction in water treatment plants using deep learning with data augmentation," *Results Eng.*, vol. 20, Dec. 2023, Art. no. 101428, doi: 10.1016/j.rineng.2023.101428.

[48] A. Dairi, F. Harrou, Y. Sun, and S. Khadraoui, "Short-term forecasting of photovoltaic solar power production using variational auto-encoder driven deep learning approach," *Appl. Sci.*, vol. 10, no. 23, p. 8400, Nov. 2020, doi: 10.3390/app10238400.

[49] B. Lim, S. Ö. Arık, N. Loeff, and T. Pfister, "Temporal fusion transformers for interpretable multi-horizon time series forecasting," *Int. J. Forecasting*, vol. 37, no. 4, pp. 1748–1764, Oct. 2021.

[50] H. H. Coban, M. Bajaj, V. Blazek, F. Jurado, and S. Kamel, "Forecasting energy consumption of electric vehicles," in *Proc. 5th Global Power, Energy Commun. Conf. (GPECOM)*, Jun. 2023, pp. 120–124, doi: 10.1109/GPECOM58364.2023.10175761.

[51] A. Jain and S. C. Gupta, "Evaluation of electrical load demand forecasting using various machine learning algorithms," *Frontiers Energy Res.*, vol. 12, pp. 1–12, Jun. 2024, doi: 10.3389/fenrg.2024.1408119.

[52] P. Boopathy, M. Liyanage, N. Deepa, M. Velavali, S. Reddy, P. K. R. Maddikunta, N. Khare, T. R. Gadekallu, W.-J. Hwang, and Q.-V. Pham, "Deep learning for intelligent demand response and smart grids: A comprehensive survey," *Comput. Sci. Rev.*, vol. 51, Feb. 2024, Art. no. 100617, doi: 10.1016/j.cosrev.2024.100617.

[53] M. Alazab, S. Khan, S. S. R. Krishnan, Q.-V. Pham, M. P. K. Reddy, and T. R. Gadekallu, "A multidirectional LSTM model for predicting the stability of a smart grid," *IEEE Access*, vol. 8, pp. 85454–85463, 2020, doi: 10.1109/ACCESS.2020.2991067.

[54] Y. Hong, Y. Zhou, Q. Li, W. Xu, and X. Zheng, "A deep learning method for short-term residential load forecasting in smart grid," *IEEE Access*, vol. 8, pp. 55785–55797, 2020, doi: 10.1109/ACCESS.2020.2981817.

[55] R. Wazirali, E. Yaghoubi, M. S. S. Abujazar, R. Ahmad, and A. H. Vakili, "State-of-the-art review on energy and load forecasting in microgrids using artificial neural networks, machine learning, and deep learning techniques," *Electr. Power Syst. Res.*, vol. 225, Dec. 2023, Art. no. 109792, doi: 10.1016/j.epsr.2023.109792.

[56] S. Islam, H. Elmekki, A. Elsebai, J. Bentahar, N. Drawel, G. Rjoub, and W. Pedrycz, "A comprehensive survey on applications of transformers for deep learning tasks," *Expert Syst. Appl.*, vol. 241, 2024, Art. no. 122666, doi: 10.1016/j.eswa.2023.122666.

[57] A. P. Jha, A. Mahajan, S. K. Singh, and P. Kumar, "Renewable energy proliferation for sustainable development: Role of cross-border electricity trade," *Renew. Energy*, vol. 201, pp. 1189–1199, Dec. 2022, doi: 10.1016/j.renene.2022.11.046.

**RITESH DASH** is currently a Research Scholar with CSE, Kalinga University, Raipur. He has a research experience of over ten years and has sound knowledge in the field of artificial intelligence, FACTS, and machine learning. He has published more than 130 numbers of research papers both in international journal and conference. Earlier, he has also published a book under CRC press. He also served the Government of India, as a Design Engineer, Electrical at WAPCOS Ltd., a Central PSU under the Ministry of Water Resources and Ganga Rejuvenation. He received the Young Engineer Award, the Madhusudan Memorial Award, and the Institutional Award from the Institution of Engineers, India. He is associated with Many international bodies, such as IEEE, Indian Science Congress, The Institution of Engineers, Solar Energy Society of India, and Carbon Society of India.

**ANUPA SINHA** is currently an Assistant Professor specializing in machine learning and artificial intelligence, with over ten years of teaching experience. She has contributed to academia through patents and book publications, focusing on innovative solutions in machine learning and AI. Her hobbies include reading research articles, mentoring students, and exploring advancements in technology for societal impact.

**K. JYOTHEESWARA REDDY** received the bachelor's degree from JNTU Kakinada, the master's degree from Sathyabama University, Chennai, and the Ph.D. degree from VIT University. He has more than seven years of teaching experience in various reputed institutions/universities. He has actively participated in all the academic and administrative activities at various levels and produced succeeded results in academia and research. He was an Associate Professor with the Sree Vidyanikethan Engineering College, Tirupati. He is currently an Associate Professor with the School of Electrical and Electronics Engineering, REVA University, Bengaluru. He has authored and co-authored more than 15 publications in reputed international journals (SCI and Scopus indexed journals) and conferences.

**C. DHANAMJAYULU** (Senior Member, IEEE) received the B.Tech. degree in electronics and communication engineering from JNTU University, Hyderabad, India, the M.Tech. degree in control and instrumentation systems from IIT Madras, Chennai, India, and the Ph.D. degree in power electronics from Vellore Institute of Technology, Vellore, India. He was invited as a Visiting Researcher with the Department of Energy Technology, Aalborg University, Esbjerg, Denmark, funded by the Danida Mobility Grant, Ministry of Foreign Affairs of Denmark on Denmark's International Development Cooperation. He was a Postdoctoral Fellow with the Department of Energy Technology, Aalborg University, from October 2019 to January 2021. He is currently an Associate Professor with Vellore Institute of Technology. His research interests include machine learning, federated learning, soft computing, computer vision, block chain, multilevel inverters, power converters, active power filters, power quality, grid connected systems, smart grids, and electric vehicle. He is recently recognized as one among the top 2% scientists in the world as per the survey conducted by Elsevier. He is an Academic Editor of the *International Transactions on Electrical Energy Systems* (Wiley), the *Mathematical Problems in Engineering* (Wiley), and the *PLOS One*, an Editorial Member of the *Scientific Reports*, an Associate Editor of the *HardwareX* and the *Journal of Electrical Engineering and Technology* (Springer), an Editorial Member of the *Discover Applied Sciences*, and an Associate Editor of the *e-prime* (Elsevier).

**INNOCENT KAMWA** (Fellow, IEEE) received the bachelor's and Ph.D. degrees in electrical engineering from Laval University, in 1985 and 1989, respectively.

He has been a Professor with the Electrical and Computer Engineering Department and the Tier 1 Canada Research Chair of the Decentralized Sustainable Electricity Grids for Smart Communities, Laval University, since September 2020. He was previously a Researcher with the Hydro-Québec's Research Institute (IREQ), where for three decades, he specialized in the dynamic performance and control of power systems from a utility perspective. Prior to his retirement from Hydro-Québec, he was successively the Chief Scientist of the Smart Grid Innovation Program, and the Acting Scientific Director and the Head of the Power System and Mathematics, responsible for the Hydro-Québec Network Simulation Centre. He was also an Adjunct Associate Professor at McGill University and Laval University, and the Product Owner and Developer of three widely used power systems simulation tools, namely EMTP, SimpowerSystems and Hypersim, commercialized by EMP Alliance, Mathworks and OPAL-RT, respectively.

Dr. Kamwa is a fellow of Canadian Academy of Engineering (CAE) and an International Member of U.S. National Academy of Engineering (NAE), "for contributions to adaptive power grid control schemes and synchronous generator testing and standards." He was a recipient of the 2019 IEEE Charles Proteus Steinmetz Technical Field Award, "for sustained leadership in the development of standards for electrical machines," and the 2019 Charles Concordia Power System Engineering Award, "for contributions in enhancing power grid performance by novel measurement devices, identification techniques, and stability control systems." He received the IEEE Power and Energy Society (PES) Distinguished Service Award, in 2013, his sustained leadership on the IEEE Power System Dynamic Performance Committee, as an AdCom Member for 15-years, and the Chair of the PES Stability Subcommittee. In parallel, he was the Treasurer and Standard Coordinator of the IEEE Electric Machinery Committee from 2006 to 2021, the Chair of IEEE Std 1110-2019, the Vice-Chair of IEEE Std 115- 2019, and the Co-Chair of IEEE Std 115-2009. He further represented IEEE PES, as a member of the IEEE Fellow Committee, and a member and the Chair of the Nikola Tesla and Herman Halperin Technical Field Awards Committees, respectively. Listed in the top 2% scientists by Stanford university, he has co-authored research articles in the top 1% most cited worldwide, leading to six IEEE PES best paper prize awards (1998, 2003, 2009, 2012, 2021, and 2022), and five IEEE PES outstanding working group awards (1998, 2006, 2011, 2013, and 2023). He was the Editor-in-Chief of *IET Generation, Transmission and Distribution* (2012–2022) and is currently the Editor-in-Chief of *IEEE Power and Energy Magazine*.